Spatiotemporal Variability of Trends and Anomaly Patterns in the Surface Albedo and Temperature of Glaciers in the Canadian Cordillera and Alaska

By

Ali Naeimi Nezamabad

A thesis submitted in partial fulfilment of the requirements for the degree of

Master of Science

Department of Earth and Atmospheric Sciences

University of Alberta

Abstract

The global average surface air temperature experienced an increase of approximately 0.5°C over the course of the 20th century. Consequently, numerous glaciers worldwide have undergone a reduction in size, and this phenomenon is especially prominent among mountain glaciers, such as those found in Western Canada and Alaska. The Canadian Cordillera and Alaska are experiencing rapid mass loss. While glacier changes have historically occurred on a time scale of centuries, recent climate-driven changes in their mass and energy balances mean that changes in glacier area, volume and runoff are now occurring on a timescale of decades.

This study aims to (i) document the spatio-temporal trends and patterns of glacier surface albedo and temperature in the Canadian Cordillera and Alaska, and (ii) evaluate physical parameters of the glaciers that experienced significant warming and darkening over the past 20 years and determine how BC deposition affects the albedo and surface temperature of snow and glacier ice surfaces across the region during the summer melt season.

Results of the study indicate that over the last 21 years, significant decreases in albedo and/or significant increases in surface temperature across 83% of the glaciated area in the study region, suggest that most of the region's glaciers are likely experiencing increasing rates of surface melting. We also found that in years with strongly significant negative surface albedo anomalies, most of the ice-covered areas had significant positive surface temperature anomalies (e.g. 2013-2019). Our findings demonstrate that the majority of the critical glaciers (warming and darkening over 21 years from 2000-2022) in the Canadian Rocky mountain area are small glaciers that are located at high elevation. Times of anomalous glacier surface albedo and temperature coincide

with years of large forest fire activity, when majority of airflow trajectories suggest that they experienced forest fire aerosol deposition, which may influence regional patterns of glacier albedo and temperature change.

Preface

A version of Chapter 2 has been published in the American Geoscience Union, Fall Meeting (AGU 2021). I was responsible for the data analyses and manuscript composition. All authors (M, Sharp, A, Dubnick) contributed to manuscript edits. I completed the study design, data analyses and manuscript composition, Aidin Niamir (Senckenberg Research Institute, Germany) assist with data analyses, M. Sharp, A. Dubnick and M. Flannigan contributed to manuscript edits.

Chapter3 is unpublished work. I completed the study design, data analyses and manuscript composition. M. Sharp, M. Flannigan and A. Dubnick contributed to manuscript edits.

Acknowledgements

Special appreciation goes to my supervisors, Dr. Martin Sharp and Dr. Mike Flannigan, for their valuable support and generous sharing of their professional and personal experiences.

I am grateful to my examination committee members, Dr. Monireh Faramarzi and Dr. Vincent St. Louise, for taking their precious time to serve on my committee. Thank you very much, Dr. Ashley Dubnick, for your friendship and invaluable scientific support throughout my program. Your assistance and insights significantly eased my journey through my projects. A special thank you to Dr. Aidin Niamir from the Data and Modelling Centre, Senckenberg Biodiversity and Climate Research Institute in Germany, for his valuable suggestions and guidance in my research direction.

I would like to express my gratitude to my lovely wife, Nesa, and my sweet son, Ryan, for their understanding, support, and love during this research period. This accomplishment would not have been possible without them.

Table of Contents

List of Tables

List of Figures

List of Appendix's

Chapter 1: Introduction

1.1 Motivation

The global mean surface air temperature rose by about 0.5°C during the 20th century (Easterling et al., 2009). As a consequence, many of the world's glaciers have shrunk (Schiermeier, 2010). This is particularly true of mountain glaciers, such as those in Western Canada and Alaska. The Canadian Cordillera and Alaska contain ~3.3 % of the world's non-polar glacier area and glaciers in these regions are experiencing rapid mass loss (Clarke, Jarosch, Anslow, Radi, Menounos, et al., 2015). Small glaciers in western Canada that are not located in deeply shaded areas are disappearing and large glaciers are warming and shrinking slightly (Christopher M. DeBeer & Sharp, 2009).

Western Canada is an essential water source for major drainage basins that impacts aquatic ecosystems and supports downstream agricultural, domestic and industrial water use, as well as hydroelectric power generation. While glacier changes have historically occurred on a time scale of centuries, recent climate-driven changes in their mass and energy balances mean that changes in glacier area, volume and runoff are now occurring on a timescale of decades (Christopher M. DeBeer & Sharp, 2009).

Coincident with the shrinking of the world's glaciers, both the total number of wildfires and the mean annual number of large wildfires in the western United States and Canada have increased over the past few decades due to climate change (Bonfils et al., 2008; Hanes et al., 2019). Within the North American Boreal region there is now a generally increasing trend in the annual area burned (Macias Fauria & Johnson, 2008). In addition to becoming more frequent, contemporary forest fires also emit more soot into the atmosphere than historical fires (Amiro et al., 2001, 2009), and this has the potential to force glacier change. A large portion of the soot emitted by forest fires is comprised of Black Carbon (BC) (Vinogradova et al., 2015).

Smoke from wildfires can temporarily reduce temperatures by a few degrees by blocking sunlight close to the Earth's surface. The smoke from wildfires can also act as a cooling agent on a global scale by enhancing the reflectivity of lower atmospheric clouds or blocking sunlight in the upper atmosphere, similar to what happens when a volcano erupts(Liu et al., 2014; Scordo et al., 2021). Light Absorbing Particles (LAPs) from North American fires may already be changing the reflectivity of glaciers in western North America (Balshi et al., 2009; Jacobson, 2004; Kroll, 2017). Black carbon deposition onto snow and ice surfaces may be efficient at increasing rates of glacier melt because the fallout season coincides with, and intensifies, the snow/ice melt season (Bond et al., 2013a). The direct (darkening) and indirect (grain-coarsening) radiative forcings associated with light-absorbing particles increase the energy available for glacier melt and are two of the largest sources of uncertainty in the modelling of regional and global climate and of the surface energy and mass balance of glaciers in the region (Skiles, S. M., Painter, 2017; Skiles et al., 2018).

The research in this chapter investigates the spatio-temporal pattern of glacier surface albedo and surface temperature change over the past 20 years and explores how the deposition of wildfire-derived BC on glaciers impacts the magnitude of the snow/ice albedo and temperature feedbacks.

1.2 Objectives and outline

The primary goals of this research are (i) to document the spatio-temporal trends and patterns of glacier surface albedo and temperature in the Canadian cordillera and Alaska (ii) to evaluate physical parameters of the glaciers that experienced significant warming and darkening over the past 20 years and determine how BC deposition affects the albedo and surface temperature of snow and glacier ice surfaces across the region during the summer melt season.

Given this background, the objectives of this research are to (1) quantify changes in the surface albedo and surface temperature of mountain glaciers in western Canada and Alaska since 2000 using data from NASA’s MODIS satellites, (2) determine the physical parameters of glaciers that are darkening and warming, as well as the impact of western Canadian wildfires black carbon (BC)

on glacier surface albedo in the Canadian Rocky mountains glaciers. These objectives are explored via a series of studies that are presented in two main chapters.

The first study (Chapter 2) quantifies recent (2000-2020) changes in surface albedo and glacier surface temperature in summertime across glaciers in the region. It explores how the glacier surface temperature and albedo dataset (2000 – 2020) for the Canadian Cordillera and Alaska was harmonized. Chapter 2 also explores spatial and temporal trends and patterns of glacier surface albedo and surface temperature since 2000 and determines (a) the magnitude of glacier surface albedo changes across the region, and (b) the spatio-temporal distribution of glacier surface temperature anomalies over the study period.

The study then examines which glaciers have reached the critical point (of having surfaces that are both warm and dark) and investigates when these states were reached and which physical parameters (surface elevation, aspect, slope, and area) had a significant influence on the time at which the critical condition for melting was reached (Chapter 3). The results from these studies will help to resolve whether and how wildfire BC deposition may affect glacier surface melt rates, meltwater production, and glacier retreat triggered by changes in glacier surface albedo and temperature within the study area over the study period.

1.3 Scientific background

Absorption of shortwave radiation is typically the largest source of energy for melting snow and ice under most atmospheric conditions (Gardner & Sharp, 2010). Snow albedo, which determines the reflection of incoming solar radiation at the snow surface, plays a vital role in the surface energy budget of snow and ice-covered regions, but is subject to large uncertainty due to the variable physical and optical properties of snow (Saito et al., 2019). A lower albedo permits more absorption of shortwave radiation, which in turn enhances warming and/or melting of the surface snow or ice cover spatiotemporal variability in the ablation areas of glaciers and ice fields (the areas in which annual surface melt exceeds the annual rate of mass accumulation on the glacier surface by snowfall). Any changes in snow albedo affect snow temperature, the melt rates of snow

and glacier ice (if exposed at the glacier surface) , and the snow cover extent (Gardner & Sharp, 2010).

Exposure of glacier ice at the glacier surface (typically by melt-induced removal of the supraglacial snow cover) is also an important influence on rates of glacier melt because the albedo of glacier ice is typically significantly lower than that of snow (Gardner & Sharp, 2010; Shafer et al., 2015; Marco Tedesco et al., 2016; Warren, 1982; Willeit & Ganopolski, 2018). Hence removal of the over-winter snowpack by spring/summer melting eventually exposes glacier ice at the glacier surface and results in a decrease in the albedo (or darkening) of lower elevation regions of glaciers in summer.

LAP's from wildfire soot and black carbon specks deposited onto or within the snowpack by precipitation or dry deposition can affect the surface albedo of a glacier. Particles deposited at the glacier surface can remain near the snow surface after deposition and continue to darken the surface until buried by new snowfall. However, during periods of intense melt, a major fraction of BC can be flushed into and/or from the snowpack via processes of meltwater scavenging (Lazarcik et al., 2017). While it is possible that some of this BC is redeposited on the glacier ice surface in downstream supraglacial environments where it can continue to affect surface albedo, most is likely to be washed downwards into the sub-surface snowpack or firn where it could (a) be buried more deeply by snowfall during the late summer or following winter (Naegeli et al., 2019; Schmale et al., 2017), (b) be exported into the glacier's ablation area, or (c) be removed from the glacier altogether by surface meltwater runoff.

The first three-dimensional global model to simulate the time-dependent spectral albedo and emissivity over snow and sea ice was developed in 2004 (Jacobson, 2004). In this model, soot that entered the snowpack via precipitation and dry deposition was found to reduce the surface albedo by 0.4% globally and by 1% in the Northern Hemisphere (Jacobson, 2004). Conway et al. (1996) showed that a reduction in snow albedo (to about 30% less than the albedo of natural snow) increased the melt rate by about 50% during experiments conducted on Snow Dome (2050 m a.s.l.) on Blue Glacier (Washington State) during July and August 1991 (Conway et al., 1996). Per unit

mass, BC has the highest solar radiation absorption of all abundant aerosols in the atmosphere (Sigl et al., 2018).

However, research in Greenland suggests there was no significant relationship between albedo reductions on the Greenland Ice Sheet and the number of fires occurring in North America from 2000 to 2016 (Marco Tedesco et al., 2016; Tedstone et al., 2017). Low albedo anomalies associated with extensive melt events have been associated with snow grain growth and an increase in surface melt rates (Shafer et al., 2015; M. Tedesco et al., 2011). In Greenland, albedo reductions in years with unusually low summer albedos have been linked to changes in atmospheric circulation and to surface melting that was amplified by atmospheric warming, as well as to algal blooms that formed on the snow surface (Tedstone et al., 2017).

Although several previous studies have identified a link between wildfires, LAP deposition on glaciers and changes in surface albedo and glacier mass balance, these studies typically use coarse resolution models and data that cover only a limited time period. Typically, they are unable to determine how orography influences the properties of the mountain snowpack and the spatial patterns of soot deposition (Ghan & Shippert, 2006; Sigl et al., 2018). The forcing depends strongly on aerosol location within the atmosphere, in particular its altitude. Internal mixing of aerosols within the atmosphere changes the forcing, and soot has large, poorly-known indirect effects (such as grain-coarsening) on snow albedo (Hansen et al., 2005). Thus, it is still uncertain how the soot-induced snow albedo perturbation affects the regional snowpack and the hydrological cycle in alpine areas, and it is difficult to model these effects because little is known about the mobility of particles in melting snow (Conway et al., 1996). Thus, it is important to obtain accurate measurements of the effect of BC on snow albedo.

1.4. Study Area

This research focuses on the glaciers of the Canadian Cordillera and Alaska. This region abuts Boreal and montane forests that have experienced significant forest fires in recent decades (Hanes et al., 2019). Most of the measured glaciers in the region have shown a coincident decline in surface mass balance (Clarke, Jarosch, Anslow, Radi, Menounos, et al., 2015) that may be partly

attributable to wildfire BC – albedo – mass balance feedbacks. The study area has a high diversity of climate and topography, and includes 37 distinct ecosystems (Christopher M. DeBeer & Sharp, 2007; Slaymaker, 2017). The study area consists of 4 ecozones; namely Alaska, Pacific Maritime, Boreal, and Montane Cordillera, which are divided in to 20 ecoregions (CEC, 1997; EPA, 2012). Lastly, glaciers in this area are of socioeconomic importance as they provide water supply for downstream irrigation, hydroelectric power production, and domestic water consumption. Thus, an understanding of the physical processes affecting glacier mass balance and meltwater runoff in the region is particularly relevant to local communities.

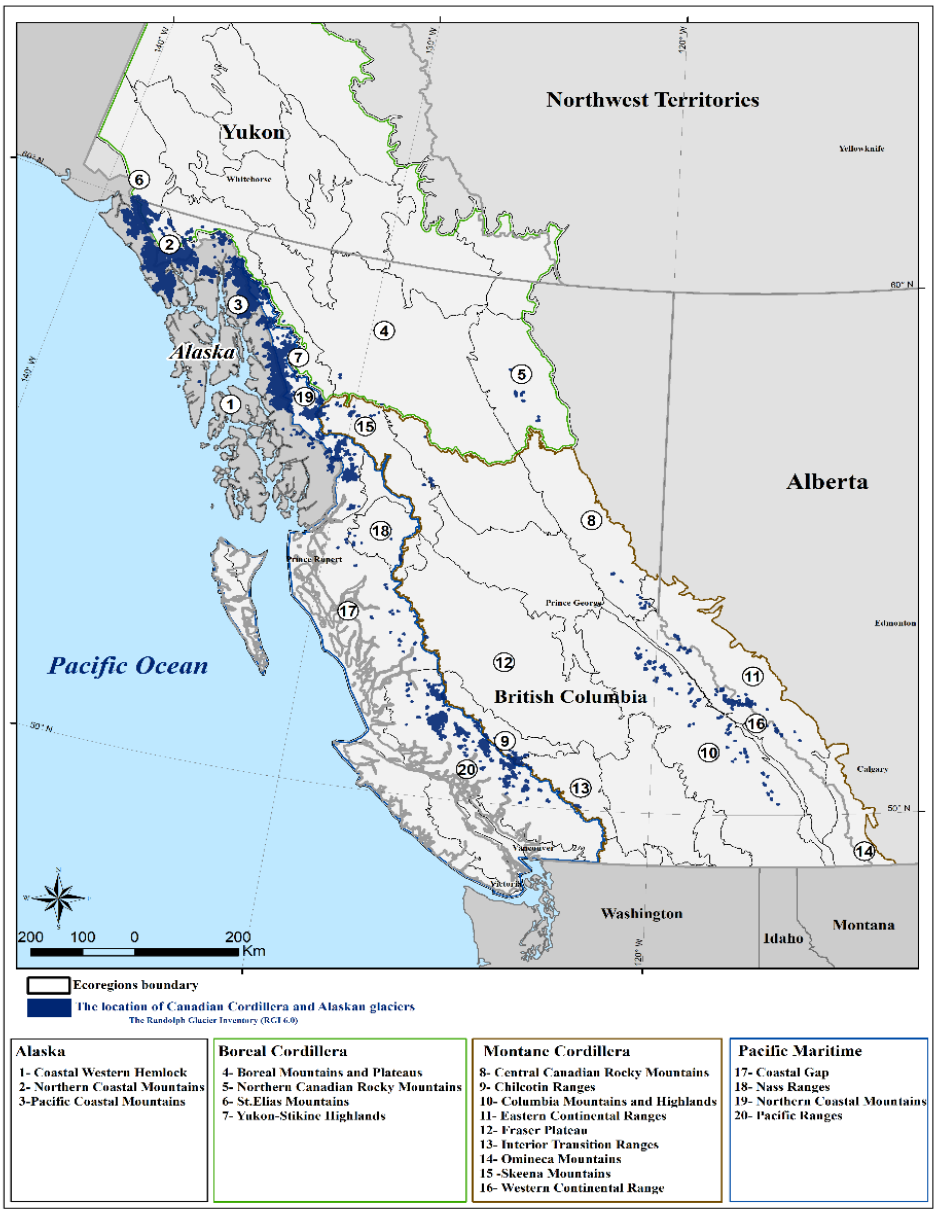

Figure 1.1: Map of study area with the 723-glacier inventory listed in the Randolph Glacier Inventory and the Canadian cordillera and southwest of Alaska ecozones (4 ecozone) and ecoregions (20 ecoregion).

Details regarding the regions are found in appendix I

Chapter 2: Harmonized glacier surface temperature and albedo dataset (2000 – 2020) of the Canadians Cordillera and Alaska

2.1 Abstract

Glacier surface albedo, a measure of the amount of solar radiation that is reflected by the glacier surface, and temperature are the primary drivers of glacier melting. Western Canada and the south of Alaska are hotspots for warming and, as a result, the magnitude of changes in the glaciers in these regions is dramatic. Knowing where and when negative trends in glacier surface albedo coincide with positive trends in glacier surface temperature is important for identifying locations and time periods in which anomalously high rates of surface melting are likely. We developed an open-source, standardized, and reproducible workflow to quantify changes in the surface albedo and surface temperature of mountain glaciers in the western Canada and southern Alaska in summertime over the 21 years from 2000 to 2020 using data from the MODIS satellites. The Randolph Glacier Inventory version 06 now includes 33 additional columns as a result of the analysis. Over the last 21 years, we observed significant decreases in albedo and/or significant increases in surface temperature across 83% of the glaciated area in the study region, suggesting most of the region's glaciers are likely experiencing increasing rates of surface melting. We also found that in years with strongly significant negative surface albedo anomalies, most of the ice-covered areas had significant positive surface temperature anomalies (e.g. 2013-2019). During the period 2000-2020, the average significant summer surface temperature over the glaciers increased by 0.026 ◦C yr−1, and the surface albedo record was negatively correlated (r: −0.86) with the surface temperature record, indicative of a positive ice-albedo feedback that would increase rates of mass loss from the western Canada and southern Alaska glaciers. Our findings demonstrate how glacier surface temperature and albedo dataset (2000 – 2020) of the Canadians Cordillera and Alaska harmonized.

2.1 Introduction

The global mean surface air temperature rose by about 0.5°C during the 20th century (Easterling et al., 2009). As a consequence, many of the world's glaciers have shrunk (Schiermeier, 2010). Similar to the vast majority of global mountain glaciers, the glaciers of the western North American mountain glaciers are rapidly melting. (Gardner et al., 2013; Kinnard et al., 2021). Over the last few decades, mountain glaciers have been losing mass due to decreases in surface albedo and increases in surface temperature. The Canadian Cordillera and Alaska contain ~3.3 % of the world's non-polar glacier area and glaciers in these regions are experiencing rapid mass loss (Clarke, Jarosch, Anslow, Radi, Menounos, et al., 2015). Surface runoff from glacier and snowmelt in western Canada is an essential water source in major drainage basins that impacts aquatic ecosystems and supports agricultural, domestic and industrial water use, and hydroelectric power generation. While glacier changes have historically occurred on a time scale of centuries, recent climate-driven changes in their mass and energy balances mean that these changes are now occurring on a timescale of decades (Christopher M. DeBeer & Sharp, 2009).

Absorption of shortwave radiation is typically the largest source of energy for melting snow and ice under most atmospheric conditions (Gardner & Sharp, 2010). On average it accounts for over 70% of the net energy input to glacier surface (Hock, 2005). Snow albedo, which determines the reflection of incoming solar radiation at the snow surface, plays a vital role in the glacier surface energy budget in snow and ice-covered regions, also dictates the seasonal variation of a glacier's surface mass balance (Saito et al., 2019; S. N. Williamson et al., 2020). A lower albedo permits more absorption of shortwave radiation, which in turn enhances warming and/or melting of the surface snow cover. Thus, the surface albedo is a dominant influence on rates of surface melt (and their spatiotemporal variability) in the ablation areas of glaciers and icefields. Any changes in snow albedo affect snow temperature, the melting of snow, and the snow cover extent (Gardner & Sharp, 2010). It is well known that the controls on the albedo of snow are complex and are due to recrystallization to larger, snow grain size, rounded grains, liquid water content in snow, solar zenith angle (SZA), and the concentrations of light-absorbing impurities both on and within the snowpack. The surface energy balance and available melt energy are strongly influenced by variations in surface albedo (Marshall & Miller, 2020).

Mountain glaciers are essential parts of the biosphere, and glacier surface temperature plays a vital role in these regions. Glacier surface temperature plays a fundamental roleon changes occurring in surface processes on alpine glaciers and is likely a better descriptor than air temperature for processes that are strongly linked to the ground surface such as cryosphere dynamics. (S. N. Williamson et al., 2014). Changes in land surface temperature (LST) provide an indication of the characteristics of the summer melt season over mountain glaciers and ice caps (Mortimer et al., 2016).

Snow and ice usually have high reflectivity, but melt can reduce the surface reflectivity significantly by lowering the surface albedo. The melted (lower albedo) surface can absorb more solar energy, which in turn increases the surface temperature (Adolph et al., 2017; He et al., 2013). Although this positive snow/ice feedback is important, it is not well quantified. Under most atmospheric conditions, the albedo and temperature of surface snow and ice are two of the main factors, controlling the energy budget glacier melting. Air temperature and precipitation are factors that control the snow and bare ice balance in the melt season. As the air temperature rise, increase glacier surface temperature and meltwater, accelerating snow metamorphism and reduction of surface temperature. Considering that surface albedo and temperature are interconnected, it is important to be aware of where and when anomalous negative albedo and positive surface temperatures coincide in order to identify locations and periods in which anomalously high rates of melting are likely to occur.

Mountain glaciers are found above the snow/tree line in regions that experience high snowfall in winter and cool temperatures in summer. Glaciers are typically difficult to access, which makes continuous in-situ observations from Automatic Weather Stations rare (Pelto et al., 2019). Local albedo and temperature are measured at a point, making it challenging to generate a high enough density of the measurements needed to create an accurate spatial coverage of a parameter that is highly spatially variable (Grenfell & Perovich, 2004). Remote sensing data and analyses of satellite images using time series methods are most efficiently able to provide useful information for glaciological applications such as estimates of glacier surface area (multi-spectral data), accumulation/ablation rates (repeat airborne or satellite laser or radar altimetry), surface albedo (e.g. MODIS spectral albedo), surface temperature (e.g. MODIS thermal infrared), equilibrium

line altitude (ELA) (e.g. multi-spectral) and the mass balance gradient (derived from repeat altimetry or in situ measurements) (Mernild et al., 2013; Rabatel et al., 2017; Racoviteanu et al., 2008; Thomas, 2001; Yuwei et al., 2014). Many geophysical data products for glaciers have been derived from Moderate Resolution Imaging Spectroradiometer (MODIS) data (including snow-cover products), because MODIS products are available globally at a spatial resolution of 250–1000 m, and with daily temporal resolution, along with 8-day composite tile products (Hall et al., 2002; Riggs & Hall, 2015; Shunlin et al., 2002). MODIS snow mapping algorithms have been automated to facilitate long term studies and have the capacity to separate most snow from clouds in order to provide reliable snow-cover information (Hall et al., 2002). Here, we use measurements from the MODIS sensors on NASA's AQUA and TERRA satellites to map the albedo and surface temperature of snow and ice on glaciers in western Canada and southern Alaska during the summer months for the period 2000-2020. We use these data to identify specific regions and time periods in which low albedo and high surface temperature coincide since these conditions are likely to result in anomalously high rates of surface melting. We also use these data to identify regions/periods in which albedo is particularly low while surface temperature is either near average or high, since such conditions suggest localized and/or short-term decoupling between the albedo and temperature of the glacier surface.

The primary objective of our study is to quantify changes in the surface albedo and surface temperature of mountain glaciers in western Canada and southern Alaska over the 21-years from 2000 to 2020 using data from the MODIS satellites. The spatial and temporal variability of anomalies in different ecoregions across the study area will be examined. This study was conducted to determine when, where, and why there are changes in surface albedo and temperature of western Canadian and southern Alaskan glaciers as these changes are important for predicting rates of mass loss from these glaciers.

2.2 Methods

2.2.1 Study area and time period

The glaciers of the Canadian Cordillera and Alaska were assessed in this study. The study area is approximately 20,000 km^2 and contains 728 alpine glaciers that occur over a range of elevations from 100 to 4600 m a.s.l. (Christopher M. DeBeer & Sharp, 2007; Slaymaker, 2017; Utama, 2017). According to Canada's Changing Climate Report published by Natural Resource Canada (NRCan) in 2019, Cordillera and south of Alaska area incorporates a variety of eco-climatic regions including Prairies, Boreal, Pacific Maritime, and Montane forests, as well as permafrost in northern and high altitude areas (Bush, E. and Lemmen, D.S, 2019). The vast majority of the study area lies within the alpine region, above 1,000 m a.s.l., while the remainder is at lower elevations in the Boreal plains or Prairies. The study area is consist of 4 ecozones; namely Alaska, Pacific Maritime, Boreal, and Montane Cordillera, which are divided in to 20 ecoregions (CEC, 1997; EPA, 2012) (Figure 1.1; see Appendix I). Our study was conducted for the 2000-2020 period, and we limited our study period to the melt season, from June to August, when incoming solar irradiance is high, solar zenith angles are low, fresh snowfall is relatively rare and both air and glacier surface temperatures are relatively high.

2.2.2 Data preparation

We obtained our glacier surface temperature dataset along with its quality control layer from MOD11A2 version 6, MODIS/Terra Land Surface Temperature and Emissivity products (LST&E) at 1 km spatial resolution for an 8-day period. For technical details of the MOD11A2 see https://lpdaac.usgs.gov/products/mod11a2v006/. This dataset was directly downloaded from the USGS Land Processes Distributed Active Archive Centre (http:/lpdaac.usgs.gov/). We obtained our glacier surface albedo dataset along with its quality assurance layer from the MOD10A1 version 6, MODIS/Terra Snow Cover Daily at 500 m spatial resolution from the National Snow and Ice Data Centre (NSDIC). For technical details of the MOD10A1 see https://nsidc.org/data/MOD10A1. All of the layers were transferred to the North America Albers Equal Area Conic (ESRI 102008) projection.

Using the quality control layer (QC_Day LST error flag) of MOD11A2, and following Mortimer et al. (2016), Riggs, and Hall (2015), we removed pixels with poor data quality (i.e. pixels with average Land Surface Temperature error equal or more than 2°C) from the glacier surface temperature dataset. For the glacier surface albedo dataset we removed pixels with a solar zenith angle higher than 70° as is recommended by NSIDC and several previous studies (Gardner & Sharp, 2010; Mortimer et al., 2018; Riggs & Hall, 2015) using the quality assurance layer (NDSI_Snow_Cover_Basic_QA) of MOD10A1. We also filtered the glacier surface albedo dataset for cloud cover pixels to ensure that non-snow albedo values (i.e. value=150) are excluded from the analysis. We obtained the glacier boundary dataset of our study area (n= 23673) from the Randolph Glacier Inventory (RGI Consortium, 2017). Considering the spatial resolution of the datasets (1 km for glacier surface temperature and 500 m for glacier surface albedo), and to harmonize with the glacier's surface areas, we removed glaciers with an area of 1 km2 or smaller from our study areas. We then removed the debris-covered area and the shadow zones. We considered the 1 km^2 inner buffer of the glacier boundary as a debris-covered area, and used ESRI ArcGIS shaded relief function (Esri, Redlands, California, USA) to calculate the shadow zones. Finally, we masked our datasets to the remaining glaciers (n = 728) and extracted the values of each pixel.

2.2.3 Data analysis

We aggregated our datasets to monthly values per glacier. To ensure reliable and even distribution of data throughout the melt season and consistency between years (Baum & Platnick, n.d.; Mortimer et al., 2016), we removed months with less than 25% observations per month (i.e. less than 2 values per month in the 8-day glacier surface temperature dataset, and less than 8 values per month in the daily glacier surface albedo dataset). The temporal trends in surface albedo and the surface temperature per glacier were calculated using linear regression to quantify variation for the period of 2000- 2020 in the study area. Cosine Similarity (CS), which measures the similarity between two sequences of numbers, was used to determine the similarity between ecoregions' mean summer glacier surface temperature and albedo. We used the linear regression coefficient to evaluate the confidence level of the trends and considered trends with less than 0.9 as insignificant. The anomalies were defined by mean values ± 1 standard deviation of each dataset

per month for a glacier. Last, we aggregated the outcome of our analysis for ecoregions and ecozones weighted by the area of each glacier. Additionally, the complete workflow described in Figure. 2.1 is highly adaptable and it can be applied to different glacier features like MODIS Snow Cover. We handled our dataset and performed our analysis using the Raster(Etten et al., 2020), Modistsp (Busetto Ranghetti, 2016), dplyr (Hadley Wickham et al., 2020), Tidyverse (Install, 2021), Broom (Package, 2021), data table (Extension et al., 2021), ggplot2 (Create et al., 2021) in R-4.0.5 (R Core Team ., 2021).

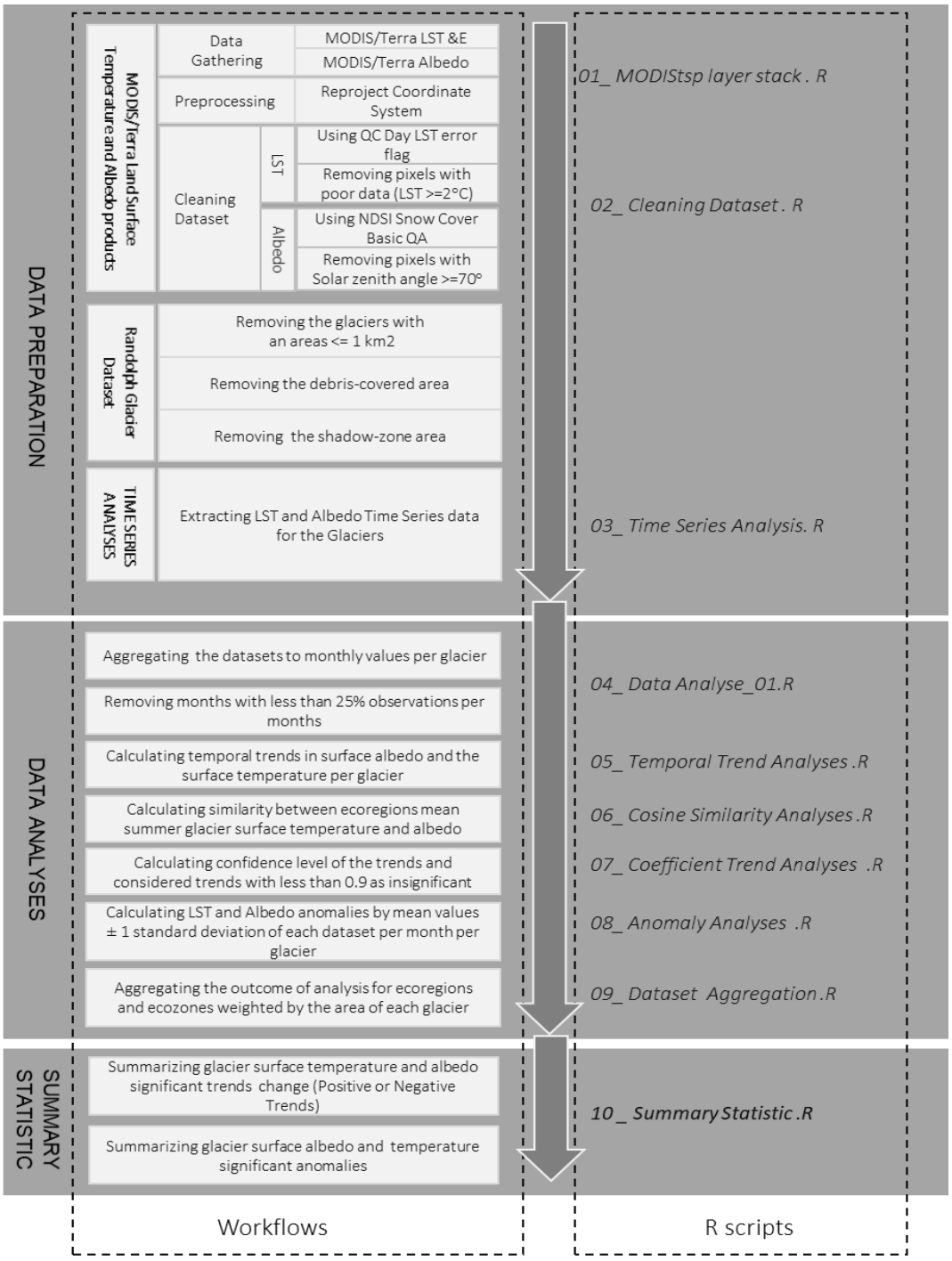

Figure 2.1: A flow chart describing the key steps of the glacier surface albedo and temperature dataset to detect trend of change and anomalies over 21 years (2000-2020).

2.2.4 Data Records

This dataset contains 57 attributes for 728 glaciers, and the data includes global glacier data (Utama, 2017) as well as aggregated data (monthly mean, monthly standard deviation) and trend analysis (monthly intercept, slope, p-value) over the past 21 years, as well as information about ecozones, ecoregions, glacier distances from the ocean, etc. The details of the collection, analysis, and interpretation of the database records can be found in appendix II.

2.3 Results

2.3.1 Glacier Surface temperature

2.3.1.1 Spatial variability in surface temperature

The mean temperature of all Canadians Cordillera and Alaskan glaciers in the melting seasons during 2000 to 2020 was 0.06°C (± 0.50°C standard deviation). The mean temperature of the glaciers of the Montane Cordillera and Alaska were relatively higher and lower, respectively in all three months of the melting session compared to other ecozones. Overall, July was the warmest month for all Canadian Cordillera and Alaskan glaciers as they all remained above the melting point (i.e. 0°C) except for glaciers in the Boreal Mountains and Plateaus ecoregion. In the Montane Cordillera ecozone, the mean temperature of the glaciers in all of the ecoregions was above 0°C during the melting session, except the Skeena Mountains ecoregion. Over the study period , the highest glacier surface temperatures were recorded in August 2004 in the Montane and Boreal Cordillera ecozones with 1.00°C (±0.20°C) and 0.81°C (±0.20°C), followed by July 2019 in the Montane Cordillera and Pacific Maritime ecozones with 0.98°C (±0.17°C) and 0.81°C (±0.30°C), (Figure 2.2; Appendix III). The glacier surface temperature patterns over study period were similar in the Alaska, Boreal Cordillera and Pacific Mountain ecozones (CS; $R \geq 0.79$), while that was not the case for the Montane Cordilleran glaciers (CS; $R \leq 0.53$) (Appendix IV).

2.3.1.2 Trends in glacier surface temperature

Overall, the trends of change in glacier surface temperature were positive in all ecozones. This shows that, in the majority of glaciated areas in all ecozones, (i.e., on average 72%) glacier surfaces were warming significantly ($p < 0.1$) in the summertime (by between 0.001°C and 2.13 °C over 21 years), (Figure. 2.3; Appendix V). The highest glaciated areas with positive significant trends in surface temperature were found in July on the Alaskan glaciers (i.e., on average 85%). In July, the majority of glaciated areas in the Alaska, the Montane Cordillera and the Pacific Maritime ecozones (i.e, ~ 73% of glaciated areas), exhibited a positive trend, while in the Boreal Cordillerian ecozone the positive trend was 57% of glaciated areas. The glaciated area's positive significant trend in June and August (i.e., an average of 64%) was lower than in July (Figure 2.3; Appendix V).

The highest average warming trend among all ecozones occurred in July (0.029 ºC yr^{-1}) and August (0.026 ºC yr^{-1}) while lowest warming trend occurred in Jun (0.025 ºC yr^{-1}). There was a large, statistically significant increase at the $p < 0.10$ level in glacier surface temperature in July (0.050 ºC yr^{-1}) in the Montane Cordillera ecoregion (Interior ranges and Skeena Mountains ecoregions), and August (0.046 ºC yr^{-1}) in the Coastal Western Hemlock ecoregion glaciers which is located in the Alaska ecozone. See figure 2.4 and appendices V for the glacier surface temperature trends plot along with their specifications. The positive glacier surface temperature trends could result in negative glacier mass balances in summertime in the absence of fresh, highly reflective snow on glacier surfaces.

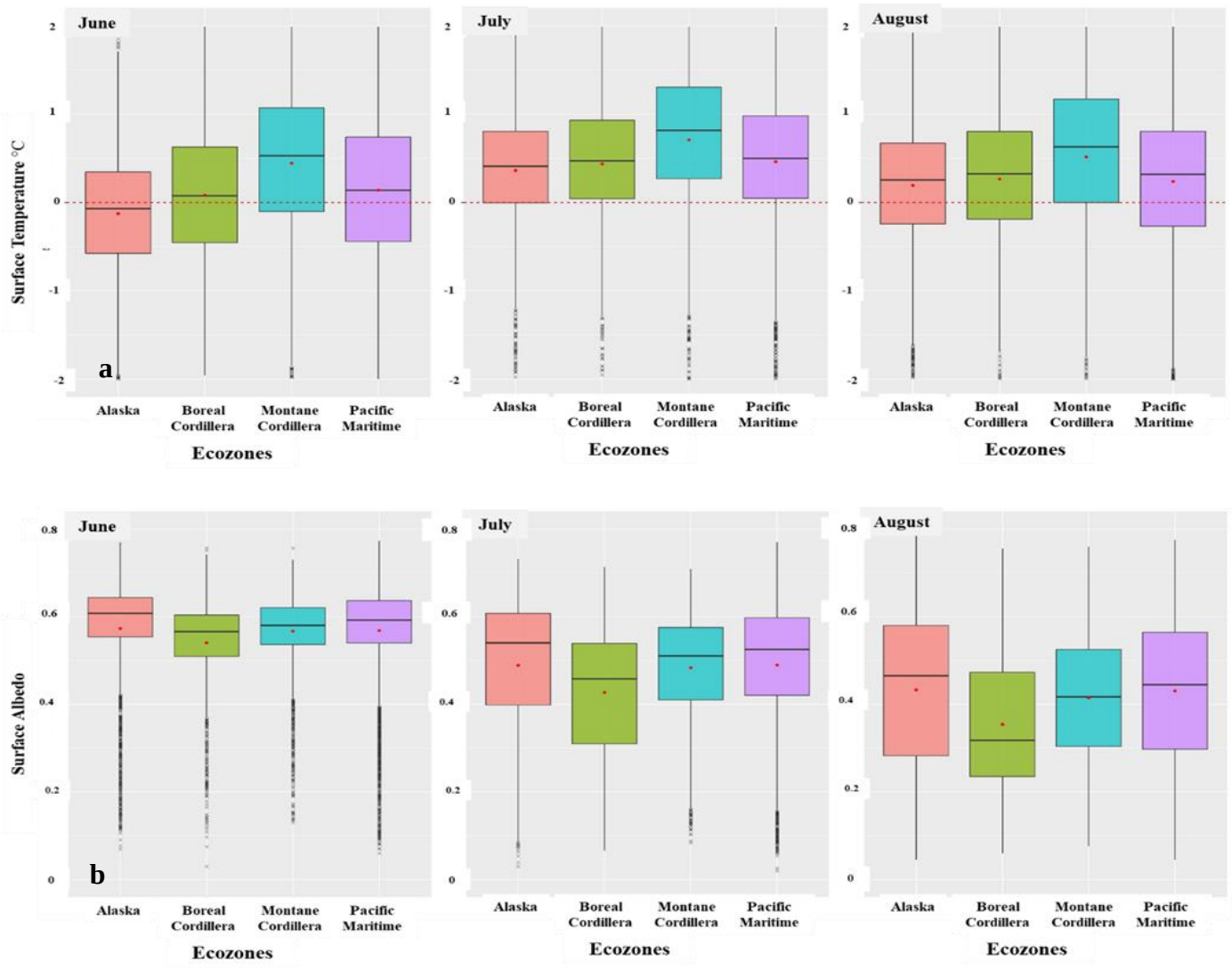

Figure 2.2: Statistical summary of (a) glacier surface temperature (°C) and glacier surface albedo (b) in the 4 main ecozones of the study area for June, July and August over 21 years (2000-2020). Boxplots indicate the median, 25th, and 75th percentiles; whiskers indicate the most extreme data points that are not considered outliers; red diamonds indicate an average; and outliers are indicated with an "×" symbol

2.3.2 Glacier surface albedo

2.3.2.1 Spatial variability in surface albedo

In the study period, the mean glacier surface albedo was relatively high with low variation in June for all Canadian Cordillera and Alaskan glaciers. In July albedo was more variable and in August it was lower. The mean glacier surface albedo was 0.48 (± 0.06 standard deviation) for all ecozones. The highest glacier surface albedo values were recorded in June 2012 (0.62 ±0.03) in the Alaskan glaciers, and the lowest value was recorded in August 2019 in the Boreal and Montane cordillera with 0.26 (±0.06 standard deviation) and 0.29 (±0.05 standard deviation), and July 2019 in the Boreal Cordillera ecozone (0.29±0.06) (Figure. 2.2; Appendix III). Cosine similarity analyses revealed that on average glacier surface albedo in all ecoregions in the study period were similar (CI; R ≥0.99) (Appendix IV).

2.3.2.2 Trends in surface albedo

In general, the majority of glaciated area's in all ecozones (in average ≥70% of glaciated area) experienced surface albedo negative significant trends ($p < 0.10$) over the study period (by between -0.03 yr^{-1} and -0.81 yr^{-1}). The highest glaciated area's with significant negative trends were observed in July and August (i.e., 75%), whereas in average 58% of the glacier areas were experienced significant negative trends in June (Figure 2.4; Appendix V).

The highest averages of significantly negative trends in glacier surface albedo in all ecozones occurred in July (-0.006 yr^{-1}) and August (-0.005 yr^{-1}) while the lowest average of significant glacier surface albedo negative trends at the $p < 0.10$ level occurred in June (-0.004 yr^{-1}). The largest statistically significant mean decreases ($p < 0.10$) in glacier surface albedo was observed in July (-0.01 yr^{-1}) in the Montane Cordillera (Columbia Mountains and Highlands ecoregions), and August (-0.08 yr^{-1}) in the Columbia Mountains and Highlands ecoregion and the Omineca Mountains ecoregion in the glaciers located in the Montane Cordillera ecozone (Figure .2.3).

2.3.3 Identification of Critical Glaciers

Using the results of trend analysis for surface albedo and surface temperature, i.e., the significant trends of $P<0.10$, we identified the most critical glaciers in the region. The glaciers experiencing negative trends (darkening) in surface albedo and positive trends (warming) in surface temperature were considered as critical glaciers.

During the months of June, July, and August, approximately 46%, 62%, and 49% of the glaciers, respectively, experienced critical significant warming and darkening over 21 years from 2000-2021 (Figure 2.4, Table, 2.1, Appendix V). The results show nearly half of glaciers in June and August and more than half of glaciers in August are absorbing more solar radiation and being warm, which can accelerate the melting process.

Table2.1: The percentage of number of glaciers with surface albedo decline (darkening) and surface temperature increase (warming) over 21-years.

Ecoregion	Significant Warming AND Darkening		
	June	July	Aug
Alaska	48.4%	73.9%	64.1%
Boreal Cordillera	57.4%	58.6%	42.9%
Montane Cordillera	41.2%	42.2%	38.7%
Pacific Maritime	38.2%	70.4%	49.3%

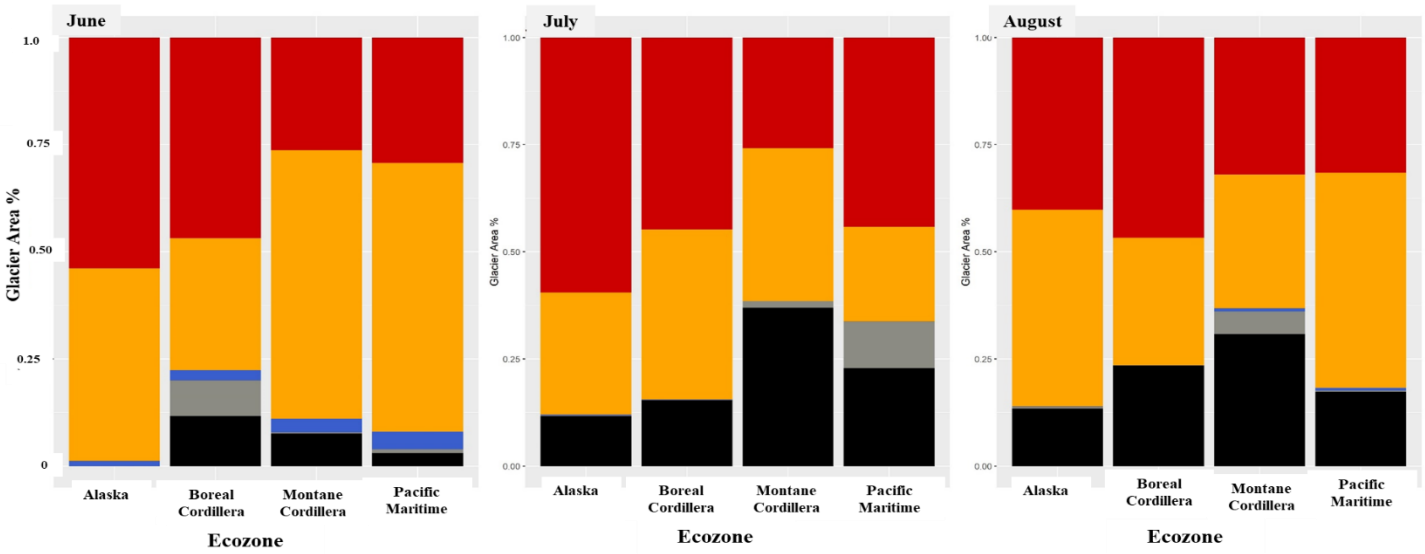

Figure 2.3: Results from the combine glacier surface temperature and albedo significant trends by glaciated areas of the four main ecozone. Red color illustrates the glaciated areas with positive significant trend in surface temperature and negative significant trend in albedo, orange color represents the glaciated areas with positive significant trend in surface temperature or negative significant trend in albedo, the blue color represents the area of glaciers the surface temperature decline and surface albedo increase, the grey color represents the glaciated areas the trends are not significant and the black color illustrates the glaciated areas with missing data

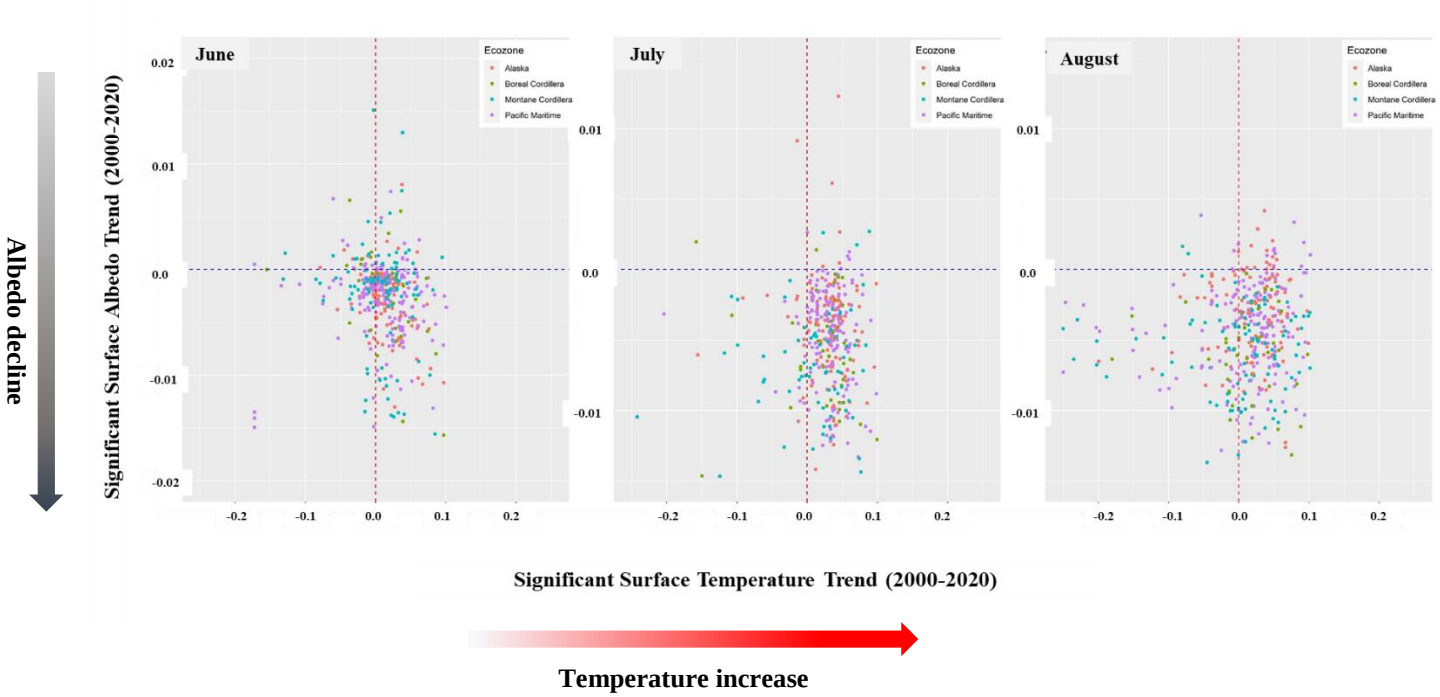

Figure 2.4: Glaciers surface albedo and temperature trends (Significant, p-value ≤ 0.1) for June-August from 2000 to 2020. The scatter plots show Significant Trends over 21-years from 2000 to 2020. The lower right quarter represents surface albedo decline (darkening) and surface temperature increase (warming) over 21-years

2.3.4 Glacier surface albedo and temperature anomalies 2000-2020

Overall, from 2000 to 2020, in the summer months, the surface temperatures of all glaciated areas were above mean-SD, except in a few years (i.e. July 2008 and August 2009 in the Boreal Cordillera and Alaska ecozones, August 2017 and June 2018 in the Boreal Cordillera ecozone, August 2020 in the Pacific Maritime ecozone, and the summer months of 2020 in the Montane Cordillera ecozone).

The highest number of significant glacier surface temperature positive anomalies at the $p \leq 0.1$ level were observed in August (i.e., 0.98°C) and July (i.e., 0.68°C), while the highest positive anomalies in June were 0.64°C on average. The highest number of glacier surface temperature positive anomalies were occurred in years 2004 (i.e., 1.91 ºC, August, Boreal Cordillera ecozone), 2013 (i.e., 1.51 ºC, August, Montane Cordillera ecozone), 2018 (i.e., 1.49 ºC, July, Pacific

Maritime ecozone), 2019 (i.e., 1.31 ºC, August, Montane Cordillera ecozone). The glacier surface temperature anomaly patterns over the study period showed the highest significant positive anomalies occurred during 2003-2006 and 2013-2016. See appendix IV for the glacier surface temperature anomalies table and plot along with their specifications.

The highest monthly average of significant negative glacier surface albedo anomaly at the $p \leq 0.1$ level was occurred in August 2019 and 2018 in the Alaska (i.e., -0.16) and Montane Cordillera (i.e., -0.15) ecozones. The highest monthly mean negative albedo anomalies in July, were observed in 2015 in the Montane and Boreal Cordilleran ecozones (i.e., -0.15) and in 2015 in the Pacific Maritime ecozone (i.e., -0.15). Regarding the glacier surface albedo anomaly analyses, the temporal variability occurred in the years 2013-2020. See appendix VI for the glacier surface temperature anomalies table.

The general patterns of significant negative surface albedo and positive surface temperature anomalies ($p < 0.05$) in the summer months were similar. In years with strongly negative surface albedo anomalies, most of the ice-covered areas had positive surface temperature anomalies (e.g. 2013-2019). In contrast, in years (i.e., 2000 and 2001 in all ecozones, 2007 and 2008 in Montane Cordillera and Pacific Maritime ecozones) glacier surface negative albedo and positive surface temperature anomalies were not negatively correlated. (Figure 2.5; Appendix VI).

However, Figure 2.5 shows glaciated areas surface temperature and surface albedo anomalies in negative correlation, also occurring surface albedo negative anomaly or positive temperature anomaly and years without anomaly.

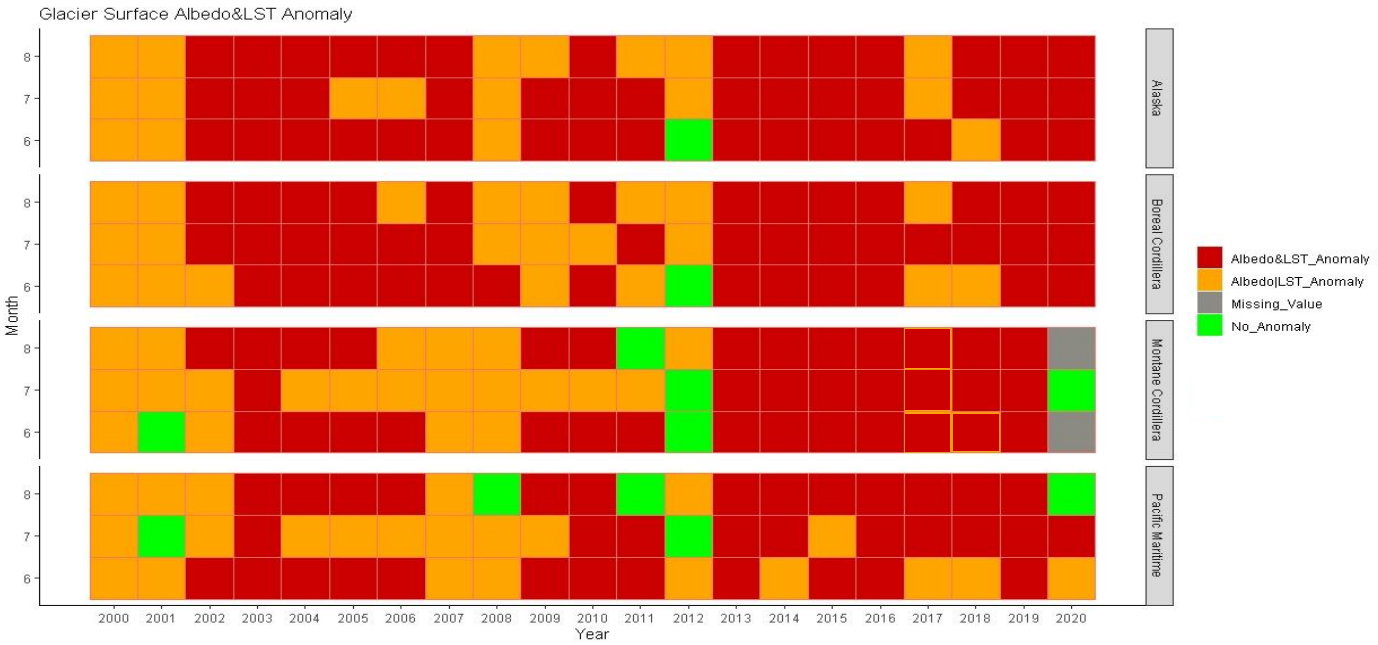

Figure 2.5: Glacier surface albedo and surface temperature anomaly relative to the 2000 – 2020 monthly mean ±1 standard deviation. **"**Red color represents glaciated areas in each ecozone with negative surface albedo AND positive surface temperature anomalies, orange color represents the glaciated areas with positive significant positive surface temperature OR negative significant anomaly in albedo, green illustrate years without significant positive surface temperature and negative significant anomaly and the grey color illustrate the glaciated areas with missing data"

2.4 Discussion

2.4.1 Summer surface albedo and temperature variability

We have presented a picture of trends and anomalies in mean summer surface albedo and surface temperature over all glaciated surfaces (with an area >1 km^2) in western Canada and the south of Alaska. This study was conducted to determine when, where, and why there are changes in the surface albedo and temperature of western Canadian and southern Alaskan glaciers as these changes are important for predicting rates of mass loss from these glaciers. Over the last 21 years, we observed significant decreases in albedo and/or significant increases in surface temperature across 83% of the studied glaciated area in the study region. The majority of the glacierized area has experienced significant warming and/or darkening in August (88% of glaciated the glacierized area) and July (83% of glaciated the glacierized area) respectively (in average 85% of the glacierized area) in the study area (Figure 2.3). Over the course of 21 years, more than half of

glaciers, varying in shape and size, have experienced significant summertime warming and darkening.

The decreases in surface albedo and increases in surface temperature of mountain glaciers that have been undergoing increased mass loss in recent decades that have been identified in this study are consistent and concurrent with the results of previous studies that have explored significant trends in the snow cover extent, glacier mass balance, surface temperature and albedo of western Canadian and Alaskan glaciers (Aubry-Wake et al., 2022; Bevington & Menounos, 2022; Clarke, Jarosch, Anslow, Radi, & Menounos, 2015; Mortimer & Sharp, 2018; S. N. Williamson & Menounos, 2021). This variability has been coincident with observed variability in air temperature anomalies, extreme warm summers, active and strong wildfire seasons and regional wildfire activity.

2.4.2 Factors contributing to changes in albedo and temperature

Many factors relating to the nature of glaciers undergoing rapid area and mass loss hinder the detection of trends in MODIS albedo at the regional-to-glacier scale. Regionally, glacier areas decline at different rates. Differences in the spatial patterns of trends in the surface albedo and surface temperature of these glaciers over the 21-year period from 2000 to 2020 reflect differences in the dominant physiographic, latitudinal, and atmospheric parameters affecting these variables. Adiabatic heating of descending air masses on the eastern and northern side of the mountain results in warm dry air, which promotes warming, melting, and enhanced albedo declines. While the western chain of mountains (Pacific Maritime and Alaska ecozones) is considered a transition zone between the polar seas of the Arctic and the temperate waters of the mid-latitude Pacific Ocean. The glaciated areas of the Pacific Maritime ecozone are situated in the wettest ecozone in Canada, receiving up to 3000 mm of precipitation per year (Ecological Stratification Working Group, 1995).

There is a strong correlation between the glacier surface temperature trends on the glaciers and the air temperature trends in summertime in the western Canada and Alaska. Positive trends in summertime glacier surface temperature that are significant at the 90% confidence level or higher

range from 0.029 ºC to 0.050 ºC per year over 21 years from 2000 to 2020 (from 0.6 ºC to 1.05 ºC) and are correlated (r=73.5) with observed changes (ºC) in annual mean air temperature between 1948 and 2016 which changed by 1.5 ºC in Canada (1.8 ºC in Prairies, 1.4 ºC in British Columbia, and 1.6 ºC in Northern Canada) in summer (Bush, E. and Lemmen, D.S, 2019). There is a strong spatial coherence in these trends, with the strongest warming occurring over western and northwestern Canada (1.5 – 3˚C) (Chris M. DeBeer et al., 2016).

The majority of Western Canadian and Alaskan glaciers have negative surface albedo and positive surface temperature anomalies in the summers of 2003-2013, 2014, 2015, 2016 and 2019 (Figure 2.5; Appendix VI). Also, it has been linked to an increase in the forested area burned over Canada, the western USA, Alaska, northern Eurasia and Siberia (cite). Concentrations of black carbon on glacier surfaces due to increased wildfire activity have been raised as a concern for glacier mass balance, due to both their direct impact on albedo and the effects of melt-albedo feedbacks (Box et al., 2012; Keegan et al., 2014; Ming et al., 2009; Tuzet et al., 2019). These wildfire conditions may have resulted in the deposition of soot and black carbon that produced the extremely low albedo values that are one of the main causes of negative anomalies in glacier BSA in the summer time (Bertoncini et al., 2020; Evangeliou et al., 2016; Kaspari et al., 2014; Kim et al., 2005; Macias Fauria & Johnson, 2008; Marshall & Miller, 2020).

2.6 Conclusions

Over the last few decades, glaciers have been losing mass due to decreases in their surface albedo and increases in their surface temperature. We employed the MODIS sensors on NASA's TERRA satellites to identify specific regions and time periods in which low surface albedo and high surface temperature coincide, since these conditions are likely to result in anomalously high rates of surface melting. The main conclusions of this study are that,

1- This study identifies the first complete picture of mean summer surface albedo and temperature and their trends and anomaly patterns over all the studied glaciated surfaces in the Canadian cordillera and southern Alaska during 2000-2020. Mean glacier summer albedo

decreased at the rate of -0.005 $yr^{-1}$and mean summer glacier surface temperature increased by 0.026 ºC yr^{-1} over the 21 years.

2- Significant negative surface albedo and/or positive surface temperature occurred over 85% of glaciated areas suggested that the majority of glaciated areas in the Canadian Cordillera and southern Alaska are darkening and warming. Declines in albedo increase the proportion of incoming solar radiation absorbed at the air–ice interface, and thus the energy available to drive melt, warming, and further surface albedo decline. Warmer temperatures, in turn, increase the rate of snow grain metamorphism, which lowers the albedo. Therefore, changes in albedo and temperature in the region are associated with a positive feedback mechanism that leads to accelerated melt.

3- The result of the research identifies years with strongly negative surface albedo anomalies, when most of the ice-covered areas had positive surface temperature anomalies (e.g. 2013-2019). The findings could suggest that glaciers in the Canadian cordillera and Alaska could melt faster than expected (Bevington & Menounos, 2022; Clarke, Jarosch, Anslow, Radi, Menounos, et al., 2015; Wood et al., 2018).

Given that, surface temperature and albedo are inextricably linked, knowing where and when albedo changes are likely to occur in the future, and factors contributing to changes in albedo and temperature are important for predicting future rates of mass loss from the Canadian Cordillera and Alaskan glaciers. Our results suggest, however, that changes occurring during the months of July and August are also important, especially as the length of the melt season continues to increase.

Chapter 3: Factors contributing to changes in albedo and temperature

3.1 Abstract

The majority of glaciers in the Canadian Rocky Mountains are expected to undergo a reduction in their net surface mass balance by the year 2100. In the Canadian Rocky Mountains, 29 glaciers with significant negative trends in surface albedo and significant positive trends in surface temperature were studied to assess whether the physical parameters of the glaciers may influence the observed trends in surface warming and darkening, and to explore whether Black Carbon from western Canadian wildfires may reduce surface albedo.

We used a Classification and Regression Tree (CART) analysis for clustering and grouping the glaciers based on physical parameters (e.g., area of glaciers, altitude, aspect and slope of the glaciers), and the Hybrid Single-Particle Lagrangian Integrated Trajectory model (HYSPLIT) was used to identify airflows that are fed by wildfire smoke and reached the study location. The majority of the critical glaciers (warming and darkening over 21 years from 2000-2022) are small glaciers (area less than 10.93 km^2) that are located at high elevation (above 2323 m.a.s.l). According to the azimuth analyses of airflow trajectories reaching the glaciers, as determined through the HYSPLIT back trajectory analysis, it was found that the majority (78%) of the airflow during the summer originated from the western region, which is recognized as a major wildfire-prone region in Canada. We also found that the mean summer surface albedo of the glaciers, averaged across the 21-year study period, was 0.49, but this dips to ~ 0.1 in some years (2003, 2015, 2017 and 2019), possibly in association with particularly active wildfire seasons in British Columbia. Times of anomalous glacier surface albedo and temperature coincide with years of large forest fire events, and majority of airflow trajectories reached to the glaciers, suggesting that forest fire aerosol deposition can influence regional patterns of glacier albedo and temperature.

3.2 Introduction

Over the past several decades, the glaciers in western North American have collectively lost mass (Clarke, Jarosch, Anslow, Radi, & Menounos, 2015; Hugonnet et al., 2021). The balance of these glaciers during the ablation season, a critical period for mass changes, is profoundly influenced by two key factors: glacier surface temperature and albedo, which represents the ratio of reflected to incident shortwave solar radiation and is expressed as a unitless quantity (Bevington & Menounos, 2022; Zhang et al., 2017).

From 2000 to 2020, the majority of mountain glaciers in western Canada and southern Alaska (83%) have experienced a decrease in surface albedo (negative significant albedo trends) and an increase in surface temperature (positive significant temperature trends) (Chapter 2). In the western Canadian mountain glaciers, the majority of glaciers fall into the category of critical, indicating that they have experienced significant decrease in albedo and increase in surface temperature. They are glaciers with an area less than 100 km^2. These glaciers are generally located at high elevations where they experience cold temperatures, which favors cold snow storage (Chapter 2).

The rate of glacier surface albedo and temperature change is affected by several physical parameters, including area, altitude, slope, and aspect (Hao et al., 2018). Slope and aspect are main physical parameters that influence glacier surface albedo and temperature since they can affect the amount of solar energy absorbed or reflected by the glacier surface. Slope and aspect also influence airflow along the glacier surface and therefore promote the drainage of cold air from high elevation to low elevation. For example, steep slopes can promote the downward advection of cold air (Houser & Hamilton, 2009) so can result in colder temperatures than those on flatter terrain.

Factors such as the deposition of black carbon (BC) from forest fires (S. N. Williamson & Menounos, 2021) (Aubry-Wake et al., 2022; Shaw et al., 2021), dust (Skiles and Painter, 2017; McGrath et al., 2018; Sarangi et al., 2019; Warren, 2013) algae (Shaw et al., 2021) can darken glacier surfaces and result in a reduced surface albedo and accelerated melt (Bond et al., 2013; S. N. Williamson & Menounos, 2021). Snow and ice surfaces tend to accumulate light-absorbing

particles during melting. (Flanner et al., 2007; Schmale et al., 2017). Once BC settles on ice sheets and high mountain glaciers, it exerts a powerful influence on their melting, as observed in regions such as Greenland, western Canada, and the Himalayas (Ghan & Shippert, 2006; Qian et al., 2015). The absorption of sunlight by BC particles warms snow which increases snow grain size (Beres et al., 2019; Qian et al., 2015). The albedo of snow is influenced by the grain size, with larger grains sizes having lower albedo, therefore hastening the melt of both snow and ice (Magalhães et al., 2019).

The total number of wildfires and the mean annual number of large wildfires in the western United States and Canada have increased over the past few decades due to climate change (Bonfils et al., 2008). Within the North American Boreal region there is now a increasing trend in the annual area burned (Macias Fauria & Johnson, 2008). Additionally, during ablation period (June, July and August), cloud cover is still low, and solar radiation is high over the Canadian Rocky mountain glaciers, which makes the deposition of solid particles, such as dust and BC (Rabatel et al., 2017) particularly influential to the energy budget of the glacier surface.

The objective of this chapter is to better understand the physical parameters that influence darkening and warming of glacier surfaces, and explore the impact that BC from western Canadian wildfires may have on glacier surface albedo in Canadian Rocky mountains glaciers. In order to achieve these objectives, we have 1) determined the glaciers within the the Canadian Rocky mountains that have experienced substantial darkening and warming, 2) defined their physical features and 3) estimated the occurrence of biomass burning in western Canada to determine the potential impact on both the surface albedo and surface temperature of mountain glaciers in the region.

3.3 Data and Methods:

3.3.1 Study area and time period

The study area consists of the glaciers of the Montane Cordillera ecozone, with emphasis to the Canadian Rocky Mountains, where significant negative trends in glacier surface albedo and

notable positive trends in surface temperatures have been observed. This region is a hotspot for warming and the magnitude of change in the glaciers in the region is dramatic. According to regional scale modeling by Clarke et al. (2015), the majority of glaciers in this area are anticipated to experience a decline in their net surface mass balance by the year 2100, creating major problems for local ecosystems, power supplies, and water quality. It is predicted that the peak glacial runoff will likely occur between 2020 and 2040 (Clarke, Jarosch, Anslow, Radi, & Menounos, 2015). The study area contains 29 alpine glaciers that occur over a range of elevations from 2200 to 3200 m a.s.l The glaciers are in 4 ecoregion: Western Continental Rages, Eastern Continental Rages, Columbia Mountains and Highlands and Central Canadian Rocky Mountains which are located in the Montane Cordillera ecozone (Figure 3.1; see Appendix VII). To examine the impact of wildfire consequence on glaciers, we limited our study period to the years in which the glacier surface were anomalously warm and dark (2017 and 2019) in summertime (June, July and August) when fresh snowfall is relatively rare and both air and glacier surface temperatures are relatively high, and when wildfires are most likely to occur.

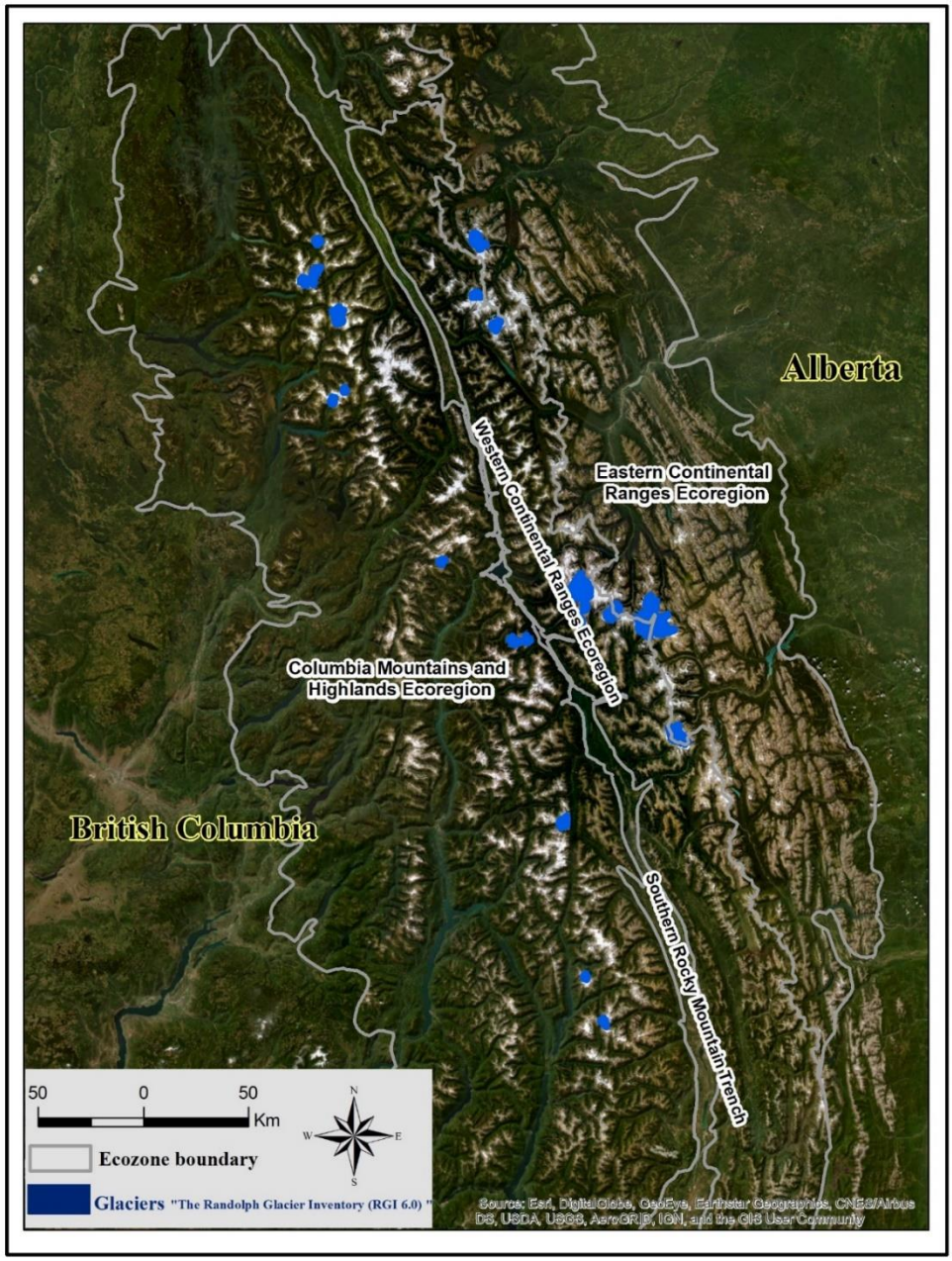

Figure 3.1: Map of the locations of 29 glaciers (with significant negative trends in surface albedo and significant positive trends in surface temperature) in the Canadian Rocky Mountain.

3.3.2 Methods

Many studies investigating glacier surges have highlighted the importance of geometrical features (Arctic Monitoring and Assessment Programme (AMAP), 2017; Bouchayer et al., 2022; Pope et al., 2016; Shaw et al., 2021). In the present study, we include the area, altitude, slope and aspect to cluster the glaciers to better understand the distribution of the glaciers in the Canadian Rocky Mountain experiencing surface darkening and warming (Appendix VII).

We used a regression tree analysis for clustering and grouping the glaciers based physical parameters and determine if the glaciers that are darkening and warming have similar physical parameters. Classification and Regression Tree (CART) Analysis is a machine learning algorithm that was used to determine the latent relationship between the glaciers and physical parameters (e.g, area of glaciers, altitude, aspect and slope of the glaciers) (Bouchayer et al., 2022).

Fitting a multivariate regression tree involves an iterative approach of cycling through a set of predictor variables. For each predictor variable, the algorithm finds a binary split that maximizes the difference among the objects with values above and below the threshold value. Following each split, the algorithm is applied to each group. The result is a tree diagram. Although the algorithm could be continued until each object (in this case, glaciers with significant negative albedo and positive temperature trends) is in its own group, a cross-validation approach is used to determine an optimal stopping point so as to avoid over-fitting the model (Basin, n.d.; McGrath et al., 2018). In this analysis, we used the rpart function in the R package to CART analyses (Partitioning & Trees, 2022).

Most of the measured glaciers in the Canadian Rocky Mountain have shown a coincident decline in surface mass balance that may be partly attributable to wildfire BC – albedo – mass balance feedbacks (Aubry-Wake et al., 2022; S. Williamson & Menounos, n.d.; S. N. Williamson & Menounos, 2021). In this research, HYSPLIT was used to identify airflows that are feed by wildfire smoke and reached to the designated study location ("HYSPLIT-4 User Guide," n.d.; Stein et al., 2015).

3.3.2.1 Tree analyses

A binary regression tree model was used to investigate the relationship between topographic and physical contexts and the presence of glacial ice areas that significantly warmed and darkened in 21 years (2000-2020). Binary regression tree models are flexible approaches that do not rely on specific assumptions, employing recursive division of information from predictor variables to minimize the sum of squared residuals within each group (Gehrke, 2011). These models serve as an alternative to assuming linear relationships between the response variable and terrain characteristics (Elder et al., 1998; Erxleben et al., 2002; Houser & Hamilton, 2009) .

Using the predictor variables, elevation, slope, aspect, and glacier area, a regression tree was grown to its maximum at 10 terminal nodes. Using cross-validation procedures and through the processes of pruning and snipping, a tree of 9^{th} terminal nodes was selected to classify the glaciers based on physical parameters. In the 9^{th} terminal node that had the lowest standard error (0.322), the aspect of glaciers didn't use and it contains the glacier's median elevation (m.a.s.l), area (Km^2) and slope (percent). By employing binary regression tree models, we were able to quantify the spatial variability in glacier distribution attributable to local terrain characteristics and explore interactions between the variables influencing ice cover distribution.

3.3.2.2 Airflow back trajectory analyses

HYSPLIT back trajectory analyses is one of the most extensively used atmospheric transport and dispersion models with the atmospheric sciences community. The model calculation technique is a combination of the Lagrangian approach and the Eulerian methodology, which employs a fixed three-dimensional grid as a reference frame to compute pollutant air concentrations (https://www.arl.noaa.gov/hysplit/).

Depending on the typical planetary boundary layer in the study area and life time of the LAP's (days to 7 days), an arrival height of 1000 m above ground level and transport duration of 7 days were used to define the arrival of pollutants from their sources of generation. The Global Data Assimilation System (GDAS) is a global atmospheric model that utilizes meteorological

measurements and numerical weather predictions to serve as meteorological input data for conducting backward air trajectory simulations. During the study period, the GDAS meteorological data covered most of the duration in a coarse resolution to minimize noise and data variability (Abreu et al., 2012). The simulation of atmospheric airflow pathways using HYSPLIT Backward Trajectory analyses focused on specific years, namely 2017 and 2019, and months within those years, specifically June, July, and August when the surface albedo was lower than the mean of the past 21 years ± the standard deviation, and the surface temperature was higher than the mean of the past 21 years ± standard deviation.

3.4 Results and discussion

3.4.1. Physical characteristics of critical glaciers

As illustrated in Figure 3.2, the binary regression tree indicates that 49% of the glaciers, totaling 14 in number, are characterized by an area of less than 10.9 km². These glaciers, classified as small, are situated at elevations exceeding 2323 meters above sea level (see Table3.1 for more details). The regression tree, as depicted in Figure 3.2 and detailed in Table 3.1, demonstrates how the interplay of four physical variables results in the identification of eight distinct environments or nodes, each contributing to the understanding of glacier distribution variance.

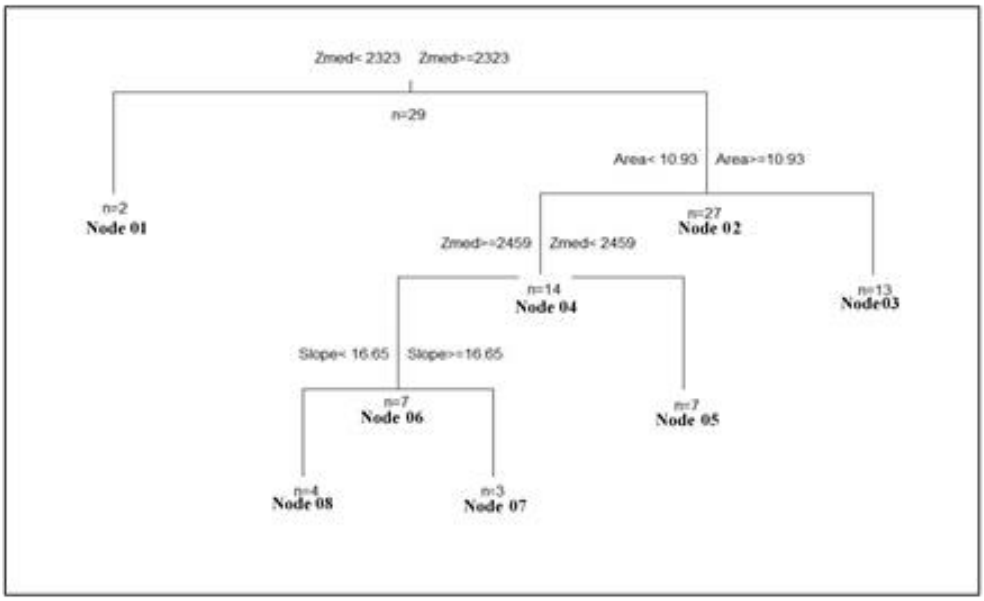

Figure 3.2. Classification and Regression Tree (CART) of glaciers (with significant negative surface albedo and positive surface temperature), in the Canadian Rocky mountain.

Table3.1: Detail information of the glaciers within each node

Nodes	Description	Number of the glaciers	Percent %	Mean warming over 21 years (+/- 1 SD)	Mean darkening over 21 years (+/- 1 SD)
Node 01	Zmed<2323	2	6.9	0.91±0.04	0.02±0.01
Node 02	Zmed>=2323	27	93.1	0.56±0.59	0.61±0.34
Node 03	Zmed>=2323 AND Area>=10.93	13	44.8	0.34±0.33	0.35±0.19
Node 04	Zmed>=2323 AND Area<10.93	14	48.3	0.22±0.26	0.26±0.15
Node 05	Zmed>=2323 AND Area<10.93 AND Zmed <2459	7	24.1	0.11±0.16	0.13±0.08
Node 06	Zmed>=2323 AND Area<10.93 AND Zmed >=2459	7	24.1	0.11±0.09	0.13±0.07
Node 07	Zmed>=2323 AND Area<10.93 AND Zmed >=2459 AND Slope>=16.65	3	10.3	0.03±0.01	0.03±0.02
Node 08	Zmed>=2323 AND Area<10.93 AND Zmed >=2459 AND Slope<16.65	4	13.8	0.07±0.08	0.10±0.05

Based on their physical characteristics, Figures 3.2 and 3.3 provide an overview of glacier clustering. The majority of glaciers experiencing darkening and warming during the 21 year record (2000-2020) are small glaciers (area less than 10.93 km^2). As shown in figure 3.2 and figure 3.3, altitude is the main parameter used to cluster glaciers because glaciers experiencing warming and

darkening are located at high elevations (mean elevation = 2541 m.a.s.l.). There are ten glaciers with north facing (n=10) and east facing (n=10) locations in the Canadian Rocky Mountains that are warming and darkening.

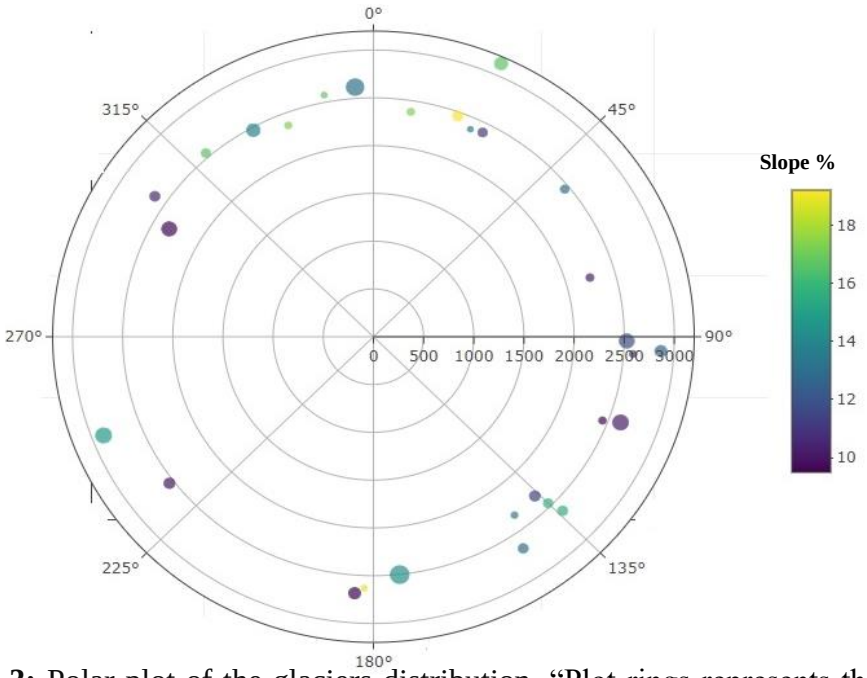

Figure 3.3: Polar plot of the glaciers distribution. "Plot rings represents the altitude, the size of the dots represents the area, the position of dots indicates the aspect, and the color of the dots signifies the slope of the glaciers"

Results from our study indicate the most pronounced warming and darkening trends were observed in smaller glaciers, specifically those with an area less than 10.93 square kilometers. Among these, the glaciers with steeper slopes and facing either north or east exhibited the highest rates of warming and darkening, as illustrated in Figure 3.3. From the 29 selected glaciers in the Canadian Rocky Mountains with significant surface temperature increase and surface albedo decrease during the past two decades (2000-2020), small glaciers facing north and east with steep slope surfaces are the most common. Figure 3.4 shows the distribution of the glaciers in different elevations regarding area, slope and aspect of the glaciers. Among the glaciers undergoing both darkening and warming, an observed spatial pattern in their physical attributes highlights the prevalence of smaller glaciers in this phenomenon. (Figure3.4, section a).

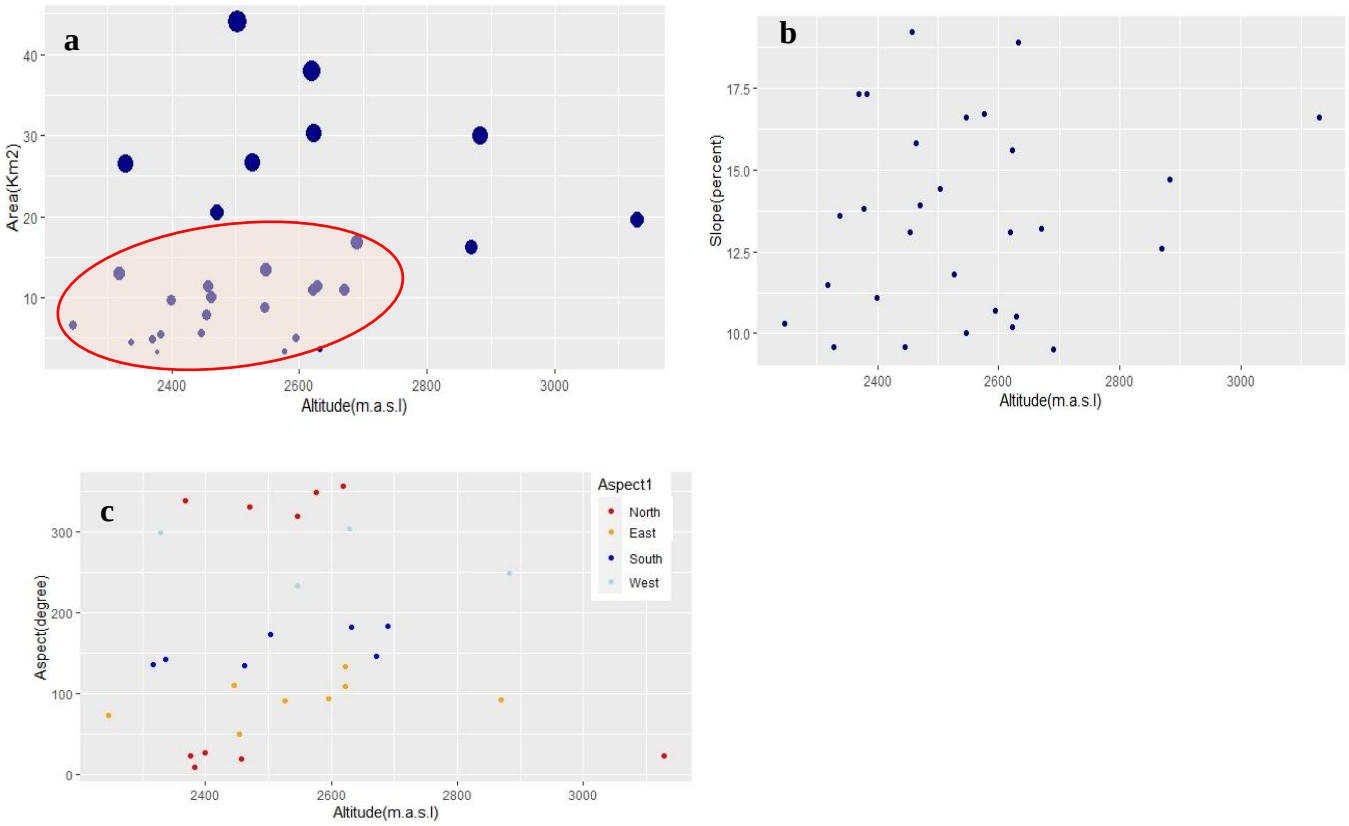

Figure 3.4: Statistical summary of glacier distributions. "(a) the distribution of glaciers with different sizes at different elevations, (b) the distribution of the glaciers slope (percent) correlated with the glacier elevation, (c) the distribution of the glacier aspects (percent) correlated with the glacier elevation"

3.4.2. Potential impact of Black Carbon

We quantified alterations on a monthly and annual basis in anomalies related to snow and ice albedo during summer for the Canadian Rocky mountain glaciers. Over the course of the 21-year period spanning 2000 to 2020, glacier surface albedo decreased by around 0.1 (over 21-years from 2000 to 2020). These declines align with years marked by heightened regional wildfire activity in western Canada, including 2003, 2015, and 2017, which recovers from this in subsequent years.

Table 3.2: The percentage of airflow trajectories reaching the glaciers as determined through Back Trajectory Analyses.

Month / Directio	June	July	August
	Percent		
North	13%	12%	14%
East	6%	5%	9%
South	5%	5%	6%
West	79%	80%	74%

Table 3.2 summarizes the findings from aggregated azimuth analyses of airflow trajectories reaching the glaciers during a 7-day period in June, July, and August for the years 2017 and 2019. According to the azimuth analyses, a significant majority (78%) of summertime airflow reaching the glaciers originated from the western region, recognized as a major wildfire-prone region in Canada (see appendix VIII for more information) (Amiro et al., 2001; Hanes et al., 2019).

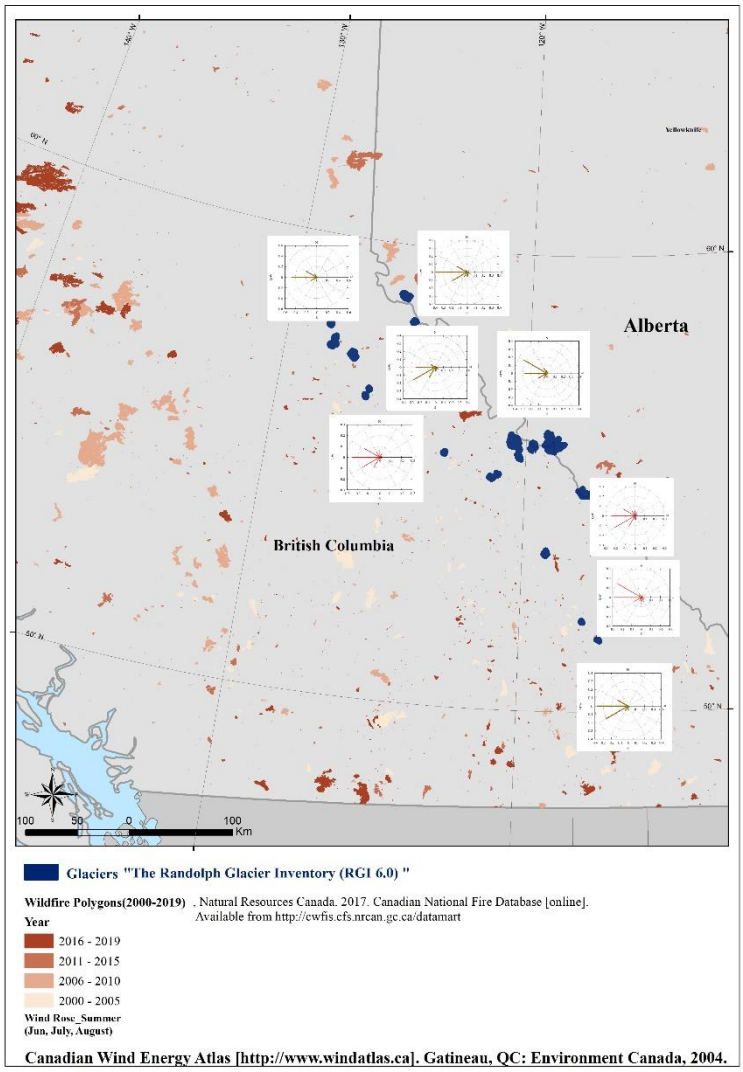

Figure3.5: The location of wildfire polygons in summertime (JJA), the glaciers with significant albedo decrease and temperature increase over 21 years (2000-2020) based the Randolph Glacier Inventory, Version 6.0, and wind-rose diagrams that are present

Based on the Canada Wind Energy Atlas (Figure 3.5), and also the Hysplit Back Trajectory Analyses (Appendix VIII, Appendix IX), it's evident that during the summer months, the prevailing wind direction over the Canadian Rocky Mountains originates from the west. This aligns with the presence of one of Canada's primary wildfire hotspots, the eastern forests of British Columbia. The mean summer surface albedo of the glaciers, averaged across the 21-year study period, was 0.49, but this dips to ~ 0.1 in some years (2003, 2015, 2017 and 2019), possibly in association with regional wildfire activity. The summers of 2003, 2017 and 2019 were particularly active wildfire seasons in British Columbia, west of the Montane Cordillera ecoregion and east of the Pacific maritime region. This could indicate that in some years during the 2000–2020 period, variability in summer wildfire activity may have influenced the glacier surface albedo anomalies.

Concentrations of black carbon on glacier surfaces due to increased wildfire activity have been raised as a concern for glacier mass balance, due to both their direct impact on albedo and the effects of melt-albedo feedbacks (Abreu et al., 2012; Dumont et al., 2014; Keegan et al., 2014; Malmros et al., 2018; Ming et al., 2009; Marco Tedesco et al., 2016). These wildfire conditions may have resulted in the deposition of soot and black carbon that produced the extremely low albedo values that are one of the main causes of negative anomalies in the glacier surface albedo in the summer time (Bertoncini et al., 2020; Evangeliou et al., 2016; Kaspari et al., 2014; Kim et al., 2005; Macias Fauria & Johnson, 2008; Marshall & Miller, 2020).

The low ice albedos measured in this study are similar to those measured on other glaciers in the Canadian Rockies during similar forest fire activity, such as on Haig Glacier, where albedo as low as 0.21 in 2003 and 2017, after summers of high forest fire activity (Marshall & Miller, 2020). It has also been discussed that decreasing surface albedo is linked to wildfire activity in the region by Williamson and Menounos (2021), who found that glacier albedo decreases over the 2000–2019 period are strongly correlated with aerosol optical depth, an indicator of smoke generated by wildfires. (S. N. Williamson & Menounos, 2021). The glaciers that have experienced the most pronounced darkening over the study are also regions that are in closest proximity to, or downstream of, intense wildfire activity.

3.5 Conclusion

We found that critical glaciers (glaciers that are significantly warming and darkening over 21 years from 2000-2020) are small glaciers that are located at high elevations. We also found that summer surface albedo was lowered during years that are characterized by intense wildfire season in western Canada where airflows reaching the glaciers are likely fed by wildfire smoke. The importance of wildfire is illustrated by the airflow trajectories reached by the glaciers from a major wildfire-prone region in Canada (British Columbia). These findings suggest that the glacier's surface albedo experiences a regional dependence on forest fire-generated light-absorbing particles.

Chapter 4: Conclusion

In recent decades, glaciers have experienced mass loss due to a decline in their surface albedo and an increase in surface temperatures in the western Canada and southern Alaska. We employed MODIS sensors on NASA's TERRA satellites to pinpoint precise regions and timeframes where low surface albedo and elevated surface temperatures coincide, as such circumstances tend to result in exceptionally high rates of surface melting. This study identifies the first complete picture of mean summer surface albedo and temperature and their trends and anomaly patterns over the glaciated surfaces in the Canadian cordillera and southern Alaska during the period 2000-2020. Specifically, the studies completed in this thesis show that:

- Significant negative surface albedo and/or positive surface temperature occurred over 85% of the glaciated area suggesting that majority of glaciated areas in the Canadian Cordillera and southern Alaska are darkening and warming. Declines in albedo increase the proportion of incoming solar radiation absorbed at the air–ice interface, and thus the energy available to drive melt, warming, and further surface albedo decline. Warmer temperatures, in turn, increase the rate of snow grain metamorphism, which lowers the albedo.
- The result of the research identifies years with strongly negative surface albedo anomalies, when most of the ice-covered areas had positive surface temperature anomalies (e.g. 2013-2019). The findings suggest that glaciers in the Canadian cordillera and Alaska could melt faster than expected
- The results identified that critical glaciers are small glaciers that are located at high elevations. The research also found that summer surface albedo was lowered during years that are characterized by intense wildfire season in western Canada where airflows reaching the glaciers are likely fed by wildfire smoke. Based on the Canada Wind Energy Atlas and the Hysplit Back Trajectory Analyses, it is also evident that during the summer months, the prevailing wind direction over the Canadian Rocky Mountains originates from the west. This aligns with the presence of one of Canada's primary wildfire hotspots, the eastern forests of British Columbia.

Given that surface temperature and albedo are inextricably linked, knowing where and when albedo changes are likely to occur in future and factors contributing to changes in albedo and temperature are important for predicting future rates of mass loss from the Canadian Cordillera and Alaskan glaciers. Our results suggest, however, that changes occurring during the months of July and August are also important, especially as the length of the melt season continues to increase.

Bibliography

Abreu, P., Aglietta, M., Ahlers, M., Ahn, E. J., Albuquerque, I. F. M., Allard, D., et al. (2012). Description of atmospheric conditions at the Pierre Auger Observatory using the Global Data Assimilation System (GDAS). *Astroparticle Physics*, *35*(9), 591–607. https://doi.org/10.1016/j.astropartphys.2011.12.002

Adolph, A. C., Albert, M. R., Lazarcik, J., Dibb, J. E., Amante, J. M., & Price, A. (2017). Dominance of grain size impacts on seasonal snow albedo at open sites in New Hampshire. *Journal of Geophysical Research*, *122*(1), 121–139. https://doi.org/10.1002/2016JD025362

Amiro, B. D., Stocks, B. J., Alexander, M. E., Flannigan, M. D., & Wotton, B. M. (2001). Fire, climate change, carbon and fuel management in the Canadian boreal forest. *International Journal of Wildland Fire*, *10*(3–4), 405–413. https://doi.org/10.1071/wf01038

Amiro, B. D., Cantin, A., Flannigan, M. D., & De Groot, W. J. (2009). Future emissions from Canadian boreal forest fires. *Canadian Journal of Forest Research*, *39*(2), 383–395. https://doi.org/10.1139/X08-154

Arctic Monitoring and Assessment Programme (AMAP). (2017). *Snow, Water, Ice and Permafrost in the Arctic (SWIPA) 2017*. *Arctic Monitoring and Assessment Programme (AMAP)*.

Aubry-Wake, C., Bertoncini, A., & Pomeroy, J. W. (2022). Fire and Ice: The impact of wildfire-affected albedo and irradiance on glacier melt. *Earth's Future*. https://doi.org/10.1029/2022ef002685

Balshi, M. S., McGuire, A. D., Duffy, P., Flannigan, M., Kicklighter, D. W., & Melillo, J. (2009). Vulnerability of carbon storage in North American boreal forests to wildfires during the 21st century. *Global Change Biology*, *15*(6), 1491–1510. https://doi.org/10.1111/j.1365-2486.2009.01877.x

Baum, B. A., & Platnick, S. (n.d.). 5 Introduction to MODIS Cloud Products.

Beres, N. D., Sengupta, D., Samburova, V., Khlystov, A. Y., & Moosmüller, H. (2019). Deposition of brown carbon onto snow: changes of snow optical and radiative properties. *Atmospheric Chemistry and Physics Discussions*, (May), 1–35. https://doi.org/10.5194/acp-2019-761

Bertoncini, A., Aubry-wake, C., & Pomeroy, J. W. (2020). Large Area High-Resolution Albedo Retrievals from Remote Sensing to Assess the Impact of Wildfire Soot Deposition on High Mountain Snow and Ice Melt . *AGU*.

Bevington, A. R., & Menounos, B. (2022). Accelerated change in the glaciated environments of western Canada revealed through trend analysis of optical satellite imagery. *Remote Sensing of Environment, 270*, 112862. https://doi.org/10.1016/j.rse.2021.112862

Bond, T. C., Doherty, S. J., Fahey, D. W., Forster, P. M., Berntsen, T., Deangelo, B. J., et al. (2013a). Bounding the role of black carbon in the climate system: A scientific assessment. *Journal of Geophysical Research Atmospheres*, *118*(11), 5380–5552. https://doi.org/10.1002/jgrd.50171

Bond, T. C., Doherty, S. J., Fahey, D. W., Forster, P. M., Berntsen, T., Deangelo, B. J., et al. (2013b). Bounding the role of black carbon in the climate system: A scientific assessment. *Journal of Geophysical Research Atmospheres*, *118*(11), 5380–5552. https://doi.org/10.1002/jgrd.50171

Bonfils, C., Santer, B. D., Pierce, D. W., Hidalgo, H. G., Bala, G., Das, T., et al. (2008). Detection and attribution of temperature changes in the mountainous Western United States. *Journal of Climate*, *21*(23), 6404–6424. https://doi.org/10.1175/2008JCLI2397.1

Bouchayer, C., Aiken, J. M., Thøgersen, K., Renard, F., & Schuler, T. V. (2022). A Machine Learning Framework to Automate the Classification of Surge-Type Glaciers in Svalbard. *Journal of Geophysical Research: Earth Surface*, *127*(7). https://doi.org/10.1029/2022JF006597

Box, J. E., Fettweis, X., Stroeve, J. C., Tedesco, M., Hall, D. K., & Steffen, K. (2012). Greenland ice sheet albedo feedback: Thermodynamics and atmospheric drivers. *Cryosphere*, *6*(4), 821–839. https://doi.org/10.5194/tc-6-821-2012

Busetto, L., & Ranghetti, L. (2016). MODIStsp: An R package for automatic preprocessing of MODIS Land Products time series. *Computers and Geosciences*, *97*, 40–48. https://doi.org/10.1016/j.cageo.2016.08.020

Bush, E. and Lemmen, D.S, E. (2019). Canada's Changing Climate Report: Temperature and Precipitation Across Canada, 112–193.

CEC. (1997). *Ecological regions of North America: toward a common perspective*.

Clarke, G. K. C., Jarosch, A. H., Anslow, F. S., Radi, V., Menounos, B., Radić, V., & Menounos, B. (2015). Projected deglaciation of western Canada in the twenty-first century. *Nature Geoscience*, *8*(5), 372–377. https://doi.org/10.1038/ngeo2407

Clarke, G. K. C., Jarosch, A. H., Anslow, F. S., Radi, V., & Menounos, B. (2015). Projected deglaciation of western Canada in the twenty-first century, (April), 6–11. https://doi.org/10.1038/NGEO2407

Conway, H., Gades, A., & Raymond, C. F. (1996). Albedo of dirty snow during conditions of melt did not persist for more than a few days . The migration of particles persisted for several weeks and , compared. *Water Resources Research*, *32*(6), 1713–1718.

Create, T., Data, E., Using, V., & Description, G. (2021). Package 'ggplot2.'

DeBeer, Chris M., Wheater, H. S., Carey, S. K., & Chun, K. P. (2016). Recent climatic, cryospheric, and hydrological changes over the interior of western Canada: A review and synthesis. *Hydrology and Earth System Sciences*, *20*(4), 1573–1598. https://doi.org/10.5194/hess-20-1573-2016

DeBeer, Christopher M., & Sharp, M. J. (2007). Recent changes in glacier area and volume within the southern Canadian Cordillera. *Annals of Glaciology*, *46*, 215–221. https://doi.org/10.3189/172756407782871710

DeBeer, Christopher M., & Sharp, M. J. (2009). Topographic influences on recent changes of very small glaciers in the Monashee Mountains, British Columbia, Canada. *Journal of Glaciology*, *55*(192), 691–700. https://doi.org/10.3189/002214309789470851

Dumont, M., Brun, E., Picard, G., Michou, M., Libois, Q., Petit, J., et al. (2014). Contribution of light-absorbing impurities in snow to Greenland ' s darkening since 2009, *7*(June), 509–512. https://doi.org/10.1038/NGEO2180

Easterling, D. R., Worthington, L. V, Hopkins, J., Stud, O., Clarke, R. A., Hill, H. W., et al. (2009). Globe Maximum and Minimum Temperature Trends for the Globe. *Science*, *277*(1997), 364–368. https://doi.org/10.1126/science.277.5324.364

Ecological Stratification Working Group. (1995). *A national ecological framework for Canada. Environment*.

Elder, K., Rosenthal, W., & Davis, R. E. (1998). Estimating the spatial distribution of snow water equivalence in a montane watershed. *Hydrological Processes*, *12*(10–11), 1793–1808. https://doi.org/10.1002/(SICI)1099-1085(199808/09)12:10/11<1793::AID-HYP695>3.0.CO;2-K

EPA. (2012). Level III Ecoregions of Texas. *Corvallis, OR*, 175. Retrieved from ftp://ftp.epa.gov/wed/ecoregions/tx/tx_eco_l3.zip, http://edg.epa.gov

Erxleben, J., Elder, K., & Davis, R. (2002). Comparison of spatial interpolation methods for estimating snow distribution in the Colorado Rocky Mountains. *Hydrological Processes*, *16*(18), 3627–3649. https://doi.org/10.1002/hyp.1239

Etten, J. Van, Sumner, M., Cheng, J., Baston, D., Bevan, A., Bivand, R., et al. (2020). Package ‘ raster ’ R topics documented :

Evangeliou, N., Balkanski, Y., Hao, W. M., Petkov, A., Silverstein, R. P., Corley, R., et al. (2016). Wildfires in northern Eurasia affect the budget of black carbon in the Arctic-a 12-year retrospective synopsis (2002-2013). *Atmospheric Chemistry and Physics*, *16*(12), 7587–7604. https://doi.org/10.5194/acp-16-7587-2016

Extension, T., Fast, D., Mpl-, L., Url, L., Needscompilation, B. T., Dowle, A. M., et al. (2021). Package ‘data.table.’

Gardner, A. S., & Sharp, M. J. (2010). A review of snow and ice albedo and the development of a new physically based broadband albedo parameterization. *Journal of Geophysical Research: Earth Surface*, *115*(1), 1–15. https://doi.org/10.1029/2009JF001444

Gardner, A. S., Moholdt, G., Cogley, J. G., Wouters, B., Arendt, A. A., Wahr, J., et al. (2013). A reconciled estimate of glacier contributions to sea level rise: 2003 to 2009. *Science*, *340*(6134), 852–857. https://doi.org/10.1126/science.1234532

Gehrke, J. (2011). Classification and Regression Trees. *Encyclopedia of Data Warehousing and Mining*, 246–280. https://doi.org/10.4018/9781591405573.ch027

Ghan, S. J., & Shippert, T. (2006). Physically based global downscaling: Climate change projections for a full century. *Journal of Climate*, *19*(9), 1589–1604. https://doi.org/10.1175/JCLI3701.1

Grenfell, T. C., & Perovich, D. K. (2004). Seasonal and spatial evolution of albedo in a snow-ice-land-ocean environment. *Journal of Geophysical Research: Oceans*, *109*(1). https://doi.org/10.1029/2003jc001866

Hadley Wickham, Romain François, Lionel Henry, & Kirill Müller. (2020). A grammar of data manipulation [R package dplyr version 1.0.0]. *Media*. Retrieved from https://cran.r-project.org/package=dplyr

Hall, D. K., Riggs, G. A., Salomonson, V. V, Digirolamo, N. E., & Bayr, K. J. (2002). MODIS snow-cover products, *83*, 181–194.

Hanes, C. C., Wang, X., Jain, P., Parisien, M. A., Little, J. M., & Flannigan, M. D. (2019). Fire-regime changes in canada over the last half century. *Canadian Journal of Forest Research*, *49*(3), 256–269. https://doi.org/10.1139/cjfr-2018-0293

Hansen, J., Sato, M., Ruedy, R., Nazarenko, L., Lacis, A., Schmidt, G. A., et al. (2005). Efficacy of climate forcings. *Journal of Geophysical Research D: Atmospheres*, *110*(18), 1–45. https://doi.org/10.1029/2005JD005776

Hao, D., Wen, J., Xiao, Q., Wu, S., Lin, X., Dou, B., et al. (2018). Simulation and analysis of the topographic effects on snow-free albedo over rugged terrain. *Remote Sensing*, *10*(2), 1–20. https://doi.org/10.3390/rs10020278

He, T., Liang, S., Yu, Y., Wang, D., Gao, F., & Liu, Q. (2013). Greenland surface albedo changes in July 1981-2012 from satellite observations. *Environmental Research Letters*, *8*(4). https://doi.org/10.1088/1748-9326/8/4/044043

Hock, R. (2005). Glacier melt: A review of processes and their modelling. *Progress in Physical Geography*, *29*(3), 362–391. https://doi.org/10.1191/0309133305pp453ra

Houser, C., & Hamilton, S. (2009). Sensitivity of post-hurricane beach. *Earth Surface Processes and Landforms*, *34*(March), 613–628. https://doi.org/10.1002/esp

Hugonnet, R., McNabb, R., Berthier, E., Menounos, B., Nuth, C., Girod, L., et al. (2021). Accelerated global glacier mass loss in the early twenty-first century. *Nature (in Press)*, *592*(July 2020). https://doi.org/10.1038/s41586-021-03436-z

HYSPLIT-4 User Guide. (n.d.).

Install, T. E. (2021). Package ‘ tidyverse ,’ 1–6.

Jacobson, M. Z. (2004). Climate response of fossil fuel and biofuel soot, accounting for soot’s feedback to snow and sea ice albedo and emissivity. *Journal of Geophysical Research D: Atmospheres*, *109*(21), 1–15. https://doi.org/10.1029/2004JD004945

Kaspari, S., Skiles, S. M., Delaney, I., Dixon, D., & Painter, T. H. (2014). Accelerated glacier melt on Snow Dome, Mount Olympus, Washington, USA, due to deposition of black carbon and mineral dust from wildfire Susan. *Nature*, *175*(4449), 238. https://doi.org/10.1038/175238c0

Keegan, K. M., Albert, M. R., McConnell, J. R., & Baker, I. (2014). Climate change and forest fires synergistically drive widespread melt events of the Greenland Ice Sheet. *Proceedings of the National Academy of Sciences*, *111*(22), 7964–7967. https://doi.org/10.1073/pnas.1405397111

Kim, Y., Hatsushika, H., Muskett, R. R., & Yamazaki, K. (2005). Possible effect of boreal wildfire soot on Arctic sea ice and Alaska glaciers. *Atmospheric Environment*, *39*(19), 3513–3520. https://doi.org/10.1016/j.atmosenv.2005.02.050

Kinnard, C., Larouche, O., Demuth, M., & Menounos, B. (2021). Mass balance modelling and climate sensitivity of Saskatchewan Glacier, western Canada. *The Cryosphere Discussions*, (April), 1–38.

Kroll, J. (2017). Fire, ice, water, and dirt: A simple climate model. *Chaos: An Interdisciplinary Journal of Nonlinear Science*, *27*(7), 073101. https://doi.org/10.1063/1.4991383

Lazarcik, J., Dibb, J. E., Adolph, A. C., Amante, J. M., Wake, C. P., Scheuer, E., et al. (2017). Major fraction of black carbon is flushed from the melting New Hampshire snowpack nearly as quickly as soluble impurities. *Journal of Geophysical Research*, *122*(1), 537–553. https://doi.org/10.1002/2016JD025351

Liu, Y., Goodrick, S., & Heilman, W. (2014). Wildland fire emissions, carbon, and climate: Wildfire-climate interactions. *Forest Ecology and Management*, *317*, 80–96. https://doi.org/10.1016/j.foreco.2013.02.020

Macias Fauria, M., & Johnson, E. A. (2008). Climate and wildfires in the North American boreal forest. *Philosophical Transactions of the Royal Society B: Biological Sciences*, *363*(1501), 2317–2329. https://doi.org/10.1098/rstb.2007.2202

Magalhães, N. de, Evangelista, H., Condom, T., Rabatel, A., & Ginot, P. (2019). Amazonian Biomass Burning Enhances Tropical Andean Glaciers Melting. *Scientific Reports*, *9*(1), 1–12. https://doi.org/10.1038/s41598-019-53284-1

Malmros, J. K., Mernild, S. H., Wilson, R., Tagesson, T., & Fensholt, R. (2018). Snow cover and snow albedo changes in the central Andes of Chile and Argentina from daily MODIS observations (2000–2016). *Remote Sensing of Environment*, *209*(February 2017), 240–252. https://doi.org/10.1016/j.rse.2018.02.072

Marshall, S., & Miller, K. (2020). Seasonal and Interannual Variability of Melt-Season Albedo at Haig Glacier, Canadian Rocky Mountains. *The Cryosphere Discussions*, (April), 1–32. https://doi.org/10.5194/tc-2020-87

McGrath, D., Sass, L., O'Neel, S., McNeil, C., Candela, S. G., Baker, E. H., & Marshall, H. P. (2018). Interannual snow accumulation variability on glaciers derived from repeat, spatially extensive ground-penetrating radar surveys. *Cryosphere*, *12*(11), 3617–3633. https://doi.org/10.5194/tc-12-3617-2018

Mernild, S. H., Pelto, M., Malmros, J. K., Yde, J. C., Knudsen, N. T., & Hanna, E. (2013). Identification of snow ablation rate, ELA, AAR and net mass balance using transient snowline variations on two arctic glaciers. *Journal of Glaciology*, *59*(216), 649–659. https://doi.org/10.3189/2013JoG12J221

Ming, J., Xiao, C., Cachier, H., Qin, D., Qin, X., Li, Z., & Pu, J. (2009). Black Carbon (BC) in the snow of glaciers in west China and its potential effects on albedos. *Atmospheric Research*, *92*(1), 114–123. https://doi.org/10.1016/j.atmosres.2008.09.007

Mortimer, C. A., & Sharp, M. (2018). Spatiotemporal variability of Canadian High Arctic glacier surface albedo from MODIS data , 2001 – 2016. *The Cryospherehere*, *12*(2), 701–720. https://doi.org/10.5194/tc-12-701-2018

Mortimer, C. A., Sharp, M., & Wouters, B. (2016). Glacier surface temperatures in the Canadian

High Arctic, 2000-15. *Journal of Glaciology*, *62*(235), 963–975. https://doi.org/10.1017/jog.2016.80

Mortimer, C. A., Sharp, M., & Vav Wychen, W. (2018). Influence of recent warming and ice dynamics on glacier surface elevations in the Canadian High Arctic, 1995–2014. *Journal of Glaciology*, *64*, 1–15. https://doi.org/10.1017/jog.2018.37

Naegeli, K., Huss, M., & Hoelzle, M. (2019). Change detection of bare-ice albedo in the Swiss Alps. *Cryosphere*, *13*(1), 397–412. https://doi.org/10.5194/tc-13-397-2019

Package, T. (2021). *Package ' broom .'*

Partitioning, T. R., & Trees, R. (2022). Package ' rpart .'

Pelto, B. M., Menounos, B., & Marshall, S. J. (2019). Multi-year Evaluation of Airborne Geodetic Surveys to Estimate Seasonal Mass Balance, Columbia and Rocky Mountains, Canada. *The Cryosphere Discussions*, 1–30. https://doi.org/10.5194/tc-2019-30

Pope, E. L., Willis, I. C., Pope, A., Miles, E. S., Arnold, N. S., & Rees, W. G. (2016). Contrasting snow and ice albedos derived from MODIS, Landsat ETM+ and airborne data from Langjökull, Iceland. *Remote Sensing of Environment*, *175*, 183–195. https://doi.org/10.1016/j.rse.2015.12.051

Qian, Y., Yasunari, T. J., Doherty, S. J., Flanner, M. G., Lau, W. K. M., Ming, J., et al. (2015). Light-absorbing particles in snow and ice: Measurement and modeling of climatic and hydrological impact. *Advances in Atmospheric Sciences*, *32*(1), 64–91. https://doi.org/10.1007/s00376-014-0010-0

Rabatel, A., Sirguey, P., Drolon, V., Maisongrande, P., Arnaud, Y., Berthier, E., et al. (2017). Annual and seasonal glacier-wide surface mass balance quantified from changes in glacier surface state: A review on existing methods using optical satellite imagery. *Remote Sensing*, *9*(5). https://doi.org/10.3390/rs9050507

Racoviteanu, A. E., Williams, M. W., & Barry, R. G. (2008). Optical remote sensing of glacier characteristics: A review with focus on the Himalaya. *Sensors*, *8*(5), 3355–3383. https://doi.org/10.3390/s8053355

RGI Consortium. (2017). Randolph Glacier Inventory--A dataset of global glacier outlines: Version 6.0. *Global Land Ice Measurements from Space, Colorado, USA, Tech. Rep*.

Riggs, G. A., & Hall, D. K. (2015). MODIS Snow Products Collection 6 User Guide, (December).

Saito, M., Yang, P., Loeb, N. G., & Kato, S. (2019). A Novel Parameterization of Snow Albedo Based on a Two-Layer Snow Model with a Mixture of Grain Habits. *Journal of the Atmospheric Sciences*, *76*(5), 1419–1436. https://doi.org/10.1175/JAS-D-18-0308.1

Sarangi, C., Qian, Y., Rittger, K., Bormann, K. J., Liu, Y., Wang, H., & Wan, H. (2019). Impact of light-absorbing particles on snow albedo darkening and associated radiative forcing over high-mountain Asia : high-resolution WRF-Chem modeling and new satellite observations, 7105–7128.

Schiermeier, Q. (2010). Glacier estimate is on thin ice: IPCC may modify its Himalayan melting forecasts. *Nature*, *463*(7279), 276. https://doi.org/10.1038/463276a

Schmale, J., Flanner, M., Kang, S., Sprenger, M., Zhang, Q., Guo, J., et al. (2017). Modulation of snow reflectance and snowmelt from Central Asian glaciers by anthropogenic black carbon. *Scientific Reports*, *7*(January), 1–10. https://doi.org/10.1038/srep40501

Scordo, F., Chandra, S., Suenaga, E., Kelson, S. J., Culpepper, J., Scaff, L., et al. (2021). Smoke from regional wildfires alters lake ecology. *Scientific Reports*, *11*(1), 1–14. https://doi.org/10.1038/s41598-021-89926-6

Shafer, M. M., Polashenski, C. M., Flanner, M. G., Dibb, J. E., Lai, A. M., Schauer, J. J., et al. (2015). Neither dust nor black carbon causing apparent albedo decline in Greenland's dry snow zone: Implications for MODIS C5 surface reflectance. *Geophysical Research Letters*, *42*(21), 9319–9327. https://doi.org/10.1002/2015gl065912

Shaw, T. E., Ulloa, G., Farías-Barahona, D., Fernandez, R., Lattus, J. M., & McPhee, J. (2021). Glacier albedo reduction and drought effects in the extratropical Andes, 1986-2020. *Journal of Glaciology*, *67*(261), 158–169. https://doi.org/10.1017/jog.2020.102

Shunlin, L., Hongliang, F., Mingzhen, C., Shuey, C. J., Charlie, W., Craig, D., et al. (2002). Validating MODIS land surface reflectance and albedo products: methods and preliminary results. *Remote Sensing of Environment*, *83*, 149–162. Retrieved from www.elsevier.com/locate/rse

Sigl, M., Abram, N. J., Gabrieli, J., Jenk, T. M., Osmont, D., & Schwikowski, M. (2018). 19th century glacier retreat in the Alps preceded the emergence of industrial black carbon deposition on high-alpine glaciers. *Cryosphere*, *12*(10), 3311–3331. https://doi.org/10.5194/tc-12-3311-2018

Skiles, S. M., Painter, T. (2017). Daily evolution in dust and black carbon content, snow grain size, and snow albedo during snowmelt, Rocky Mountains, Colorado. *Journal of Glaciology*, *63*(237), 118–132. https://doi.org/10.1017/jog.2016.125

Skiles, S. M. K., Flanner, M., Cook, J. M., Dumont, M., & Painter, T. H. (2018). Radiative forcing by light-absorbing particles in snow. *Nature Climate Change*, *8*(11), 964–971. https://doi.org/10.1038/s41558-018-0296-5

Slaymaker, O. (2017). *Landscapes and Landforms of Western Canada*. Springer. https://doi.org/10.1007/978-3-319-44595-3

Stein, A. F., Draxler, R. R., Rolph, G. D., Stunder, B. J. B., Cohen, M. D., & Ngan, F. (2015). Noaa's hysplit atmospheric transport and dispersion modeling system. *Bulletin of the American Meteorological Society*, *96*(12), 2059–2077. https://doi.org/10.1175/BAMS-D-14-00110.1

Tedesco, M., Fettweis, X., Van Den Broeke, M. R., Van De Wal, R. S. W., Smeets, C. J. P. P., Van De Berg, W. J., et al. (2011). The role of albedo and accumulation in the 2010 melting record in Greenland. *Environmental Research Letters*, *6*(1). https://doi.org/10.1088/1748-9326/6/1/014005

Tedesco, Marco, Doherty, S., Fettweis, X., Alexander, P., Jeyaratnam, J., & Stroeve, J. (2016). The darkening of the Greenland ice sheet: Trends, drivers, and projections (1981-2100). *Cryosphere*, *10*(2), 477–496. https://doi.org/10.5194/tc-10-477-2016

Tedstone, A. J., Bamber, J. L., Cook, J. M., Williamson, C. J., Fettweis, X., Hodson, A. J., & Tranter, M. (2017). Dark ice dynamics of the south-west Greenland Ice Sheet. *Cryosphere*, *11*(6), 2491–2506. https://doi.org/10.5194/tc-11-2491-2017

Thind, P. S., Kumar, D., & John, S. (2021). Source apportionment of the light absorbing impurities present in surface snow of the India Western Himalayan glaciers. *Atmospheric Environment*, *246*(December 2020), 118173. https://doi.org/10.1016/j.atmosenv.2020.118173

Thomas, R. H. (2001). Remote sensing reveals shrinking greenland ice sheet. *Eos*, *82*(34), 369–373. https://doi.org/10.1029/01EO00226

Tuzet, F., Dumont, M., Arnaud, L., Voisin, D., Lamare, M., Larue, F., et al. (2019). Influence of light absorbing particles on snow spectral irradiance profiles, (April), 1–33.

Utama, aditia edy. (2017). 1Randolph Glacier Inventory –A Dataset of Global Glacier Outlines: Version6.0, (July), 1–14.

Vinogradova, A. A., Smirnov, N. S., Korotkov, V. N., & Romanovskaya, A. A. (2015). Forest fires in Siberia and the Far East: Emissions and atmospheric transport of black carbon to the Arctic. *Atmospheric and Oceanic Optics*, *28*(6), 566–574. https://doi.org/10.1134/S1024856015060184

Warren, S. G. (1982). optical properties of snow by Warren 1982.pdf. *Review of Geophysics and Space Physics*, *20*(1), 67–89.

Warren, S. G. (2013). Can black carbon in snow be detected by remote sensing? *Journal of Geophysical Research Atmospheres*, *118*(2), 779–786. https://doi.org/10.1029/2012JD018476

Willeit, M., & Ganopolski, A. (2018). The importance of snow albedo for ice sheet evolution over the last glacial cycle. *Climate of the Past*, *14*(5), 697–707. https://doi.org/10.5194/cp-14-697-2018

Williamson, S., & Menounos, B. (n.d.). Trends , Patterns and Influences of Glacier Albedo , Western North America.

Williamson, S. N., & Menounos, B. (2021). The influence of forest fires aerosol and air temperature on glacier albedo, western North America. *Remote Sensing of Environment*, *267*(September), 112732. https://doi.org/10.1016/j.rse.2021.112732

Williamson, S. N., Hik, D. S., Gamon, J. A., Kavanaugh, J. L., & Flowers, G. E. (2014). Estimating temperature fields from MODIS land surface temperature and air temperature observations in a sub-arctic alpine environment. *Remote Sensing*, *6*(2), 946–963. https://doi.org/10.3390/rs6020946

Williamson, S. N., Copland, L., Thomson, L., & Burgess, D. (2020). Comparing simple albedo scaling methods for estimating Arctic glacier mass balance. *Remote Sensing of Environment*, *246*(May), 111858. https://doi.org/10.1016/j.rse.2020.111858

Wood, W. H., Marshall, S. J., & Fargey, S. E. (2018). of the Canadian Rocky Mountains , 2005-2010, (June), 1–24.

Yuwei, W. U., Jianqiao, H. E., Zhongming, G., & Anan, C. (2014). Limitations in identifying the equilibrium-line altitude from the optical remote-sensing derived snowline in the Tien Shan, China. *Journal of Glaciology*, *60*(224), 1117–1125. https://doi.org/10.3189/2014JoG13J221

Zhang, Y., Kang, S., Cong, Z., Schmale, J., Sprenger, M., Li, C., et al. (2017). Light-absorbing impurities enhance glacier albedo reduction in the southeastern Tibetan plateau. *Journal of Geophysical Research*, *122*(13), 6915–6933. https://doi.org/10.1002/2016JD026397

Appendix

Appendix I, Overview of number of glaciers and sample points in the study.

Ecozone	Ecoregion	*Number of glaciers	Area ($Km^{2)}$	**Number of sample points	Elevation (m)				***Aspect
					Min	Max	Range	Average	
Alaska	Coastal Western Hemlock	15	41	192	88	1589	1500	671	SE
	Northern Coastal Mountains	38	564	742	723	3062	2339	1530	SE
	Pacific Coastal Mountains	111	10115	6405	256	3010	2754	1254	SE
	Total	**164**	**10720**	**7339**					
Boreal Cordillera	Boreal Mountains and Plateaus	3	17	3	1998	2438	439	2164	W
	Northern Canadian Rocky Mountains	14	84	46	2143	2481	338	2250	S
	St.Elias Mountains	19	1709	1072	544	1883	1338	1362	SE
	Yukon-Stikine Highlands	27	255	86	1391	2101	711	1683	SE
	Total	**65**	**2064**	**1207**					
Montane Cordillera	Central Canadian Rocky Mountains	11	69	26	1809	2617	808	2134	SE
	Chilcotin Ranges	20	166	102	1442	2618	1176	2286	S
	Columbia Mountains and Highlands	78	503	235	2160	2811	652	2440	S
	Eastern Continental Ranges	28	343	187	2370	3159	789	2710	SE
	Fraser Plateau	2	11	3	1840	1965	125	1894	SW
	Interior Transition Ranges	6	40	10	1967	2252	285	2160	E
	Omineca Mountains	7	39	25	1751	2041	291	1967	SW
	Skeena Mountains	20	125	109	1290	2046	757	1721	SW
	Western Continental Ranges	28	312	185	2096	3106	1010	2559	SE
	Total	**202**	**1606**	**882**					
Pacific Maritime	Coastal Gap	21	107	46	1028	1972	945	1621	SE
	Nass Ranges	11	58	26	1472	2034	562	1737	SE
	Northern Coastal Mountains	139	2823	4026	1042	2078	1036	1660	SE
	Pacific Ranges	126	2510	1052	1447	2641	1194	2029	SE
	Total	**297**	**5499**	**5150**					

* Glaciers with an area of at least 1 km2 or one (M∗D11A1) to four (M∗D10A1) MODIS pixels
** The number of Modis pixel values used to extract glacier surface albedo and surface temperature
*** Mean aspect of glacier area; each aspect value (N, NE, E, SE, S, SW, W, NE) represents an aspect interval of 45º

Appendix II, Description of fields of the dataset.

Column ID	Full name	Description	Format	Unit
RGIID	Randolph Glacier Inventory Identifier	The identifying code of each glacier	Character	
ZONE_NAME	Ecozone Name	An area with very board physiograic and ecological similarity	Character	
REGION_NAM	Ecoregion Name	An area with very board physiograic and ecological similarity within each Ecozone	Character	
Number_Sample		The number of sample points to extract data for analyses in each glacier	Numeric	
GLIMSId	Global Land Ice Measurements from Space initiative	The identifying code of each glacier	Character	
BgnDate	Begin Date	The date of the source from which the outline was taken	Date	
EndDate	End Date	The date of the source from which the outline was taken	Date	
CenLon	CenLon	Single point representing the location (Longitude) of the glacier	Numeric	Degree
CenLat	CenLat	Single point representing the location (Latitude) of the glacier	Numeric	Degree
O1Region	O1Region	The codes of the first-order regions to which the glacier belongs.		
O2Region	O2Region	The codes of the second order regions to which the glacier belongs.		
Zmin	Zmin	Minimum elevation of the glacier	Numeric	Meter above sea level
Zmax	Zmax	Maximum elevation of the glacier	Numeric	Meter above sea level
Zmed	Zmed	Median elevation of the glacier,	Numeric	Meter above sea level
Slope	Slope	Mean slope of the glacier surface	Numeric	Degree
Aspect	Aspect	The aspect of the glacier surface	Numeric	Degree
Lmax	Lmax	Length of the longest surface flow line of the glacier	Numeric	Meter
Status	Status			
Form	Form	Form of the ice body(e.g. Glacier, Ice cap, perennial snowfield, seasonal snowfield and not assigned)	Numeric	
TermType	TermType	Terminus type of glaciers (e.g. Land, marine and lake terminating, dry calving,regenerated, shelf terminated and not assigned)	Numeric	
Surging	Surging	Information on evidence for surging (e.g. no evidence, possible, probable, observed and not assigned)	Numeric	
Linkages	Linkages	Status of link to mass-balance measurements in the World Glacier Monitoring Service	Numeric	
Name	Name	Name of the glacier		
Area_Km	Area_Km	Area of the glacier in km2	Numeric	
Dis2_Pacific_MIN	Minimum distance to Pacific Ocean	The glacier minimum distance to the Pacific Ocean	Numeric	Meter

Dis2_Pacific_MAX	Maximum distance to Pacific Ocean	The glacier maximum distance to the Pacific Ocean	Numeric	Meter
Dis2_Pacific_MEAN	Mean distance to Pacific Ocean	The glacier average distance to the Pacific Ocean	Numeric	Meter
LST_intercept_June	Land Surface Temperature Intercept in June	The predicted value for land surface temperature, when x is 0.	Numeric	Degree Celsius
LST_Slope_June	Land Surface Temperature slope in June	The average rate of land surface temperature change or steepness of a line over 21 years	Numeric	Degree Celsius
LST_P.Value_June	Land Surface Temperature Probablity Value in June	A statistical test to determine the significance of Land Surface Temperature linear regression results in relation to the null hypothesis.	Numeric	
LST_intercept_July	Land Surface Temperature Intercept in July	The predicted value for land surface temperature, when x is 0.	Numeric	Degree Celsius
LST_Slope_July	Land Surface Temperature slope in July	The average rate of land surface temperature change or steepness of a line over 21 years	Numeric	Degree Celsius
LST_P.Value_July	Land Surface Temperature Probablity Value in July	A statistical test to determine the significance of Land Surface Temperature linear regression results in relation to the null hypothesis.	Numeric	
LST_intercept_Aug	Land Surface Temperature Intercept in August	The predicted value for land surface temperature, when x is 0.	Numeric	Degree Celsius
LST_Slope_Aug	Land Surface Temperature slope in August	The average rate of land surface temperature change or steepness of a line over 21 years	Numeric	Degree Celsius
LST_P.Value_Aug	Land Surface Temperature Probablity Value in August	A statistical test to determine the significance of Land Surface Temperature linear regression results in relation to the null hypothesis.	Numeric	
Albedo_intercept_Jun	Albedo Intercept in June	The predicted value for Albedo, when x is 0.	Numeric	uniteless(%) *
Albedo_Slope_Jun	Albedo slope in June	The average rate of Albedo change or steepness of a line over 21 years	Numeric	uniteless(%) *
Albedo_P.Value_Jun	Albedo Probablity Value in June	A statistical test to determine the significance of Albedo linear regression results in relation to the null hypothesis.	Numeric	
Albedo_intercept_July	Albedo Intercept in July	The predicted value for Albedo, when x is 0.	Numeric	uniteless(%) *
Albedo_Slope_July	Albedo slope in July	The average rate of Albedo change or steepness of a line over 21 years	Numeric	uniteless(%) *
Albedo_P.Value_July	Albedo Probablity Value in July	A statistical test to determine the significance of Albedo linear regression results in relation to the null hypothesis.	Numeric	
Albedo_intercept_Aug	Albedo Intercept in August	The predicted value for Albedo, when x is 0.	Numeric	uniteless(%) *
Albedo_Slope_Aug	Albedo slope in August	The average rate of Albedo change or steepness of a line over 21 years	Numeric	uniteless(%) *
Albedo_P.Value_Aug	Albedo Probablity Value in August	A statistical test to determine the significance of Albedo linear regression results in relation to the null hypothesis.	Numeric	
LST_Mean_Jun	Land Surface Temperature Mean in June	Glacier Surface Temperature average in June over 21 years (2000-2020)	Numeric	Degree Celsius

LST_SD_Jun	Land Surface Temperature Standard Deviation in June	Glacier Surface Temperature is clustered (Low standard deviation) or spread out (high standard deviation) around the mean in June over 21 years (2000-2020)	Numeric	Degree Celsius
LST_Mean_July	Land Surface Temperature Mean in July	Glacier Surface Temperature average in July over 21 years (2000-2020)	Numeric	Degree Celsius
LST_SD_July	Land Surface Temperature Standard Deviation in July	Glacier Surface Temperature is clustered (Low standard deviation) or spread out (high standard deviation) around the mean in July over 21 years (2000-2020)	Numeric	Degree Celsius
LST_Mean_Aug	Land Surface Temperature Mean in August	Glacier Surface Temperature average in August over 21 years (2000-2020)	Numeric	Degree Celsius
LST_SD_Aug	Land Surface Temperature Standard Deviation in August	Glacier Surface Temperature is clustered (Low standard deviation) or spread out (high standard deviation) around the mean in August over 21 years (2000-2020)	Numeric	Degree Celsius
Albedo_Mean_Jun	Albedo Mean in June	Glacier Surface Albedo average in June over 21 years (2000-2020)	Numeric	uniteless(%)*
Albedo_SD_Jun	Albedo Standard Deviation in June	Glacier Surface Albedo is clustered (Low standard deviation) or spread out (high standard deviation) around the mean in June over 21 years (2000-2020)	Numeric	uniteless(%)*
Albedo_Mean_July	Albedo Mean in July	Glacier Surface Albedo average in July over 21 years (2000-2020)	Numeric	uniteless(%)*
Albedo_SD_July	Albedo Standard Deviation in July	Glacier Surface Albedo is clustered (Low standard deviation) or spread out (high standard deviation) around the mean in July over 21 years (2000-2020)	Numeric	uniteless(%)*
Albedo_Mean_Aug	Albedo Mean in August	Glacier Surface Albedo average in August over 21 years (2000-2020)	Numeric	uniteless(%)*
Albedo_SD_Aug	Albedo Standard Deviation in August	Glacier Surface Albedo is clustered (Low standard deviation) or spread out (high standard deviation) around the mean in August over 21 years (2000-2020)	Numeric	uniteless(%)*

*percentage or a decimal value, with 1 being a perfect reflector and 0 absorbing all incoming light

Appendix III, The average and standard deviation of the glacier surface albedo and surface temperature °C in the 4 main ecozones of the study area for June, July and August over 21 years (2000-2020)

Land Surface Temperature °C																								
	Alaska						**Boreal Cordillera**						**Montane cordillera**						**Pacific Maritime**					
	June		July		August		June		July		August		June		July		August		June		July		August	
	Mean	±SD	Mean	±SD	Mean	±SD	Mean	±SD	Mean	±SD	Mean	±SD	Mean	±SD	Mean	±SD	Mean	±SD	Mean	±SD	Mean	±SD	Mean	±SD
2000	-0.03	0.97	0.19	0.86	-0.23	1.48	0.11	0.90	0.41	0.86	0.25	1.24	0.64	0.71	1.06	0.53	0.19	1.18	0.20	0.95	0.35	0.80	-0.54	1.62
2001	-0.38	1.32	0.30	1.18	-0.33	1.75	-0.35	1.14	0.15	1.55	-0.43	2.06	-0.08	1.35	0.39	1.28	-0.62	1.40	-0.24	1.25	-0.10	1.65	-0.78	2.04
2002	-0.52	1.40	0.29	1.04	-0.17	1.69	-0.51	1.53	0.25	1.07	-0.71	1.60	-0.36	1.37	0.76	0.84	0.28	1.24	-0.20	1.22	0.39	0.82	-0.42	1.42
2003	0.00	0.94	0.55	0.86	-0.05	1.12	0.21	0.82	0.39	0.83	0.10	1.01	0.47	0.91	0.67	0.73	0.71	0.78	0.19	0.79	0.50	0.78	-0.01	1.13
2004	0.31	0.91	0.41	1.02	0.45	1.05	0.38	1.03	0.64	0.60	0.94	0.66	0.67	0.88	0.42	0.94	1.01	0.51	0.49	0.92	0.32	0.94	0.64	0.77
2005	0.24	0.88	-0.24	1.40	0.24	1.25	0.53	0.63	-0.08	1.10	0.25	0.86	0.71	0.67	0.00	1.14	0.01	1.19	0.28	0.90	-0.06	1.24	0.11	0.98
2006	-0.04	0.96	0.35	0.94	-0.09	1.13	0.08	0.92	0.50	0.74	0.22	0.95	0.70	0.84	0.22	0.91	-0.02	1.55	0.28	0.81	0.18	1.02	-0.37	1.46
2007	-0.45	1.07	0.05	1.50	0.13	1.01	-0.16	1.25	0.32	0.61	0.44	0.80	0.42	0.87	0.56	0.86	0.35	1.19	-0.24	1.17	0.14	1.12	-0.08	1.03
2008	-0.65	1.71	-0.42	1.48	-0.94	2.02	-0.07	1.11	-0.97	1.88	-0.74	1.81	0.11	1.23	0.16	1.31	-0.88	2.02	-0.22	1.06	-0.28	1.52	-1.34	2.22
2009	-0.34	1.34	0.71	0.62	-1.25	2.81	0.01	1.05	0.63	0.68	-3.10	4.42	0.53	0.97	0.84	0.49	-0.33	1.74	0.19	0.92	0.62	0.60	-1.50	2.89
2010	-0.53	1.27	0.37	1.02	0.43	0.91	-0.36	1.36	0.14	1.02	0.36	0.71	0.43	0.79	0.24	1.09	0.73	0.90	-0.34	1.18	0.35	0.84	0.01	1.17
2011	-0.54	1.87	0.17	1.10	-0.16	1.11	-0.48	1.89	0.25	0.95	-0.57	1.44	0.25	1.33	0.32	0.93	-0.06	1.54	-0.11	1.39	0.22	0.96	-0.58	1.50
2012	-0.70	1.07	0.21	1.02	-0.20	1.35	-0.51	1.24	0.10	1.36	0.11	1.17	0.05	1.16	0.02	1.13	0.73	0.91	-0.27	1.10	0.04	1.27	0.10	1.33
2013	-0.09	1.31	0.48	0.95	-0.39	1.44	0.02	1.34	0.56	0.74	0.16	1.10	0.41	0.92	0.43	0.57	0.78	0.74	-0.10	1.34	0.60	0.81	0.33	1.34
2014	-0.14	1.21	0.65	0.80	0.30	1.01	0.36	0.88	0.55	0.84	0.17	0.88	0.46	0.95	0.53	0.76	0.42	1.12	0.15	0.99	0.60	0.74	0.17	0.98
2015	0.43	0.69	0.29	1.17	0.00	1.07	0.45	0.64	0.40	1.03	0.11	1.12	0.65	0.60	0.31	1.01	0.33	0.92	0.51	0.83	-0.05	1.29	0.14	1.00

2016	0.04	0.96	0.32	1.19	-0.10	1.18	0.24	0.85	0.16	0.93	0.27	0.84	0.33	1.17	-0.52	0.98	0.50	1.12	0.23	0.91	0.29	1.14	0.17	1.02
2017	-0.58	1.29	-0.25	1.87	-0.66	2.56	-0.19	1.27	-0.74	1.60	-1.23	3.13	0.32	1.04	0.66	0.88	-1.24	2.71	-0.29	1.55	0.08	1.12	-1.13	2.64
2018	-1.09	1.89	0.80	0.80	0.10	1.22	-1.05	1.79	0.84	0.92	-0.17	1.32	-0.17	1.41	1.10	0.59	0.33	0.79	-1.08	2.11	0.82	0.71	0.19	1.00
2019	0.35	1.05	-0.27	1.54	0.43	0.86	0.51	0.86	-0.05	1.11	0.53	0.78	0.64	0.92	-0.08	1.07	0.92	0.62	0.41	0.99	0.22	1.21	0.50	0.84
2020	-0.68	1.37	0.48	0.98	-0.05	1.19	-0.04	1.04	0.15	1.16	-0.03	1.24	-0.63	1.40	-0.11	1.19	-1.52	1.72	-0.58	1.20	-0.22	1.28	-1.74	1.86
Average	**0.57**	**0.07**	**0.49**	**0.08**	**0.43**	**0.10**	**0.54**	**0.06**	**0.43**	**0.08**	**0.35**	**0.09**	**0.57**	**0.05**	**0.48**	**0.06**	**0.42**	**0.07**	**0.57**	**0.04**	**0.49**	**0.06**	**0.43**	**0.07**

Land Surface Albedo																								
	Alaska						**Boreal Cordillera**						**Montane cordillera**						**Pacific Maritime**					
	June		July		August		June		July		August		June		July		August		June		July		August	
	Mean	±SD	Mean	±SD	Mean	±SD	Mean	±SD	Mean	±SD	Mean	±SD	Mean	±SD	Mean	±SD	Mean	±SD	Mean	±SD	Mean	±SD	Mean	±SD
2000	0.61	0.06	0.57	0.07	0.52	0.10	0.61	0.04	0.55	0.07	0.45	0.10	0.61	0.04	0.57	0.05	0.51	0.07	0.61	0.03	0.57	0.04	0.51	0.07
2001	0.63	0.05	0.55	0.07	0.50	0.09	0.60	0.05	0.51	0.07	0.42	0.08	0.62	0.04	0.55	0.06	0.49	0.06	0.62	0.04	0.55	0.04	0.49	0.06
2002	0.57	0.06	0.51	0.08	0.45	0.10	0.54	0.05	0.45	0.09	0.37	0.08	0.57	0.04	0.52	0.06	0.45	0.07	0.57	0.03	0.53	0.05	0.47	0.06
2003	0.52	0.07	0.43	0.09	0.40	0.10	0.47	0.06	0.37	0.07	0.33	0.07	0.54	0.04	0.45	0.07	0.38	0.07	0.54	0.04	0.45	0.06	0.42	0.07
2004	0.56	0.05	0.48	0.08	0.40	0.10	0.55	0.04	0.42	0.08	0.32	0.09	0.54	0.04	0.44	0.06	0.35	0.06	0.56	0.03	0.47	0.06	0.40	0.08
2005	0.57	0.07	0.50	0.10	0.41	0.11	0.54	0.06	0.43	0.09	0.33	0.09	0.57	0.05	0.51	0.07	0.41	0.07	0.56	0.04	0.50	0.07	0.42	0.07
2006	0.58	0.06	0.51	0.08	0.44	0.11	0.56	0.05	0.45	0.07	0.37	0.09	0.58	0.04	0.53	0.06	0.44	0.08	0.57	0.03	0.51	0.05	0.43	0.08
2007	0.60	0.06	0.53	0.07	0.45	0.09	0.58	0.05	0.47	0.08	0.36	0.08	0.60	0.04	0.55	0.06	0.48	0.07	0.58	0.03	0.54	0.05	0.48	0.06
2008	0.59	0.06	0.53	0.08	0.48	0.10	0.58	0.05	0.47	0.07	0.40	0.08	0.59	0.04	0.52	0.06	0.49	0.07	0.59	0.04	0.52	0.05	0.49	0.06
2009	0.59	0.05	0.50	0.08	0.44	0.09	0.58	0.04	0.45	0.07	0.37	0.08	0.59	0.04	0.50	0.06	0.42	0.06	0.59	0.03	0.51	0.05	0.45	0.06
2010	0.59	0.06	0.50	0.08	0.44	0.10	0.56	0.06	0.43	0.08	0.34	0.09	0.57	0.05	0.49	0.06	0.41	0.07	0.58	0.04	0.49	0.05	0.41	0.07

2011	0.57	0.07	0.50	0.08	0.44	0.10	0.52	0.07	0.41	0.08	0.36	0.10	0.56	0.05	0.49	0.06	0.44	0.08	0.57	0.04	0.50	0.06	0.45	0.07
2012	0.64	0.04	0.58	0.07	0.55	0.09	0.62	0.04	0.57	0.05	0.49	0.09	0.62	0.03	0.56	0.05	0.52	0.07	0.62	0.03	0.57	0.03	0.53	0.06
2013	0.59	0.06	0.47	0.10	0.43	0.10	0.56	0.06	0.39	0.09	0.32	0.09	0.57	0.05	0.46	0.06	0.40	0.07	0.57	0.04	0.47	0.06	0.41	0.07
2014	0.56	0.08	0.44	0.10	0.40	0.10	0.53	0.07	0.39	0.08	0.33	0.09	0.58	0.05	0.48	0.07	0.41	0.07	0.56	0.05	0.48	0.06	0.42	0.07
2015	0.52	0.08	0.45	0.09	0.39	0.10	0.46	0.07	0.37	0.08	0.32	0.08	0.52	0.06	0.44	0.06	0.36	0.07	0.53	0.05	0.46	0.06	0.40	0.07
2016	0.56	0.08	0.46	0.10	0.40	0.11	0.50	0.07	0.38	0.09	0.31	0.09	0.55	0.06	0.45	0.07	0.35	0.08	0.54	0.05	0.44	0.07	0.38	0.08
2017	0.56	0.08	0.46	0.10	0.41	0.10	0.51	0.08	0.41	0.08	0.34	0.09	0.56	0.05	0.46	0.07	0.39	0.08	0.57	0.05	0.47	0.06	0.40	0.08
2018	0.54	0.08	0.40	0.10	0.37	0.10	0.49	0.08	0.32	0.08	0.30	0.08	0.54	0.07	0.38	0.07	0.32	0.07	0.53	0.06	0.38	0.07	0.35	0.07
2019	0.49	0.08	0.38	0.09	0.34	0.09	0.42	0.08	0.30	0.07	0.27	0.07	0.47	0.06	0.34	0.06	0.29	0.06	0.48	0.06	0.38	0.07	0.33	0.07
2020	0.59	0.07	0.50	0.09	0.43	0.12	0.57	0.07	0.43	0.08	0.35	0.11	0.59	0.05	0.49	0.06	0.41	0.08	0.59	0.04	0.49	0.06	0.44	0.10
Average	**-0.26**	**1.21**	**0.26**	**1.11**	**-0.12**	**1.39**	**-0.04**	**1.12**	**0.22**	**1.03**	**-0.15**	**1.39**	**0.31**	**1.02**	**0.38**	**0.92**	**0.12**	**1.23**	**-0.04**	**1.12**	**0.24**	**1.04**	**-0.29**	**1.44**

Figures

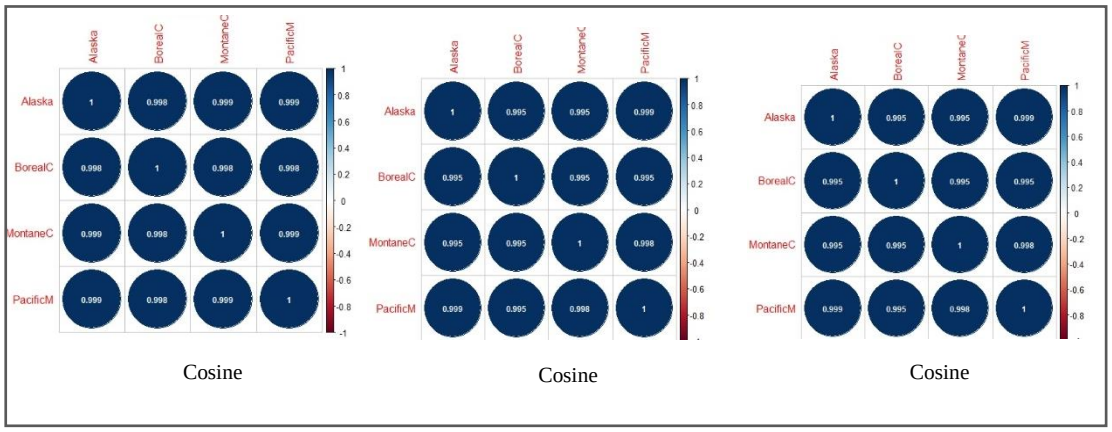

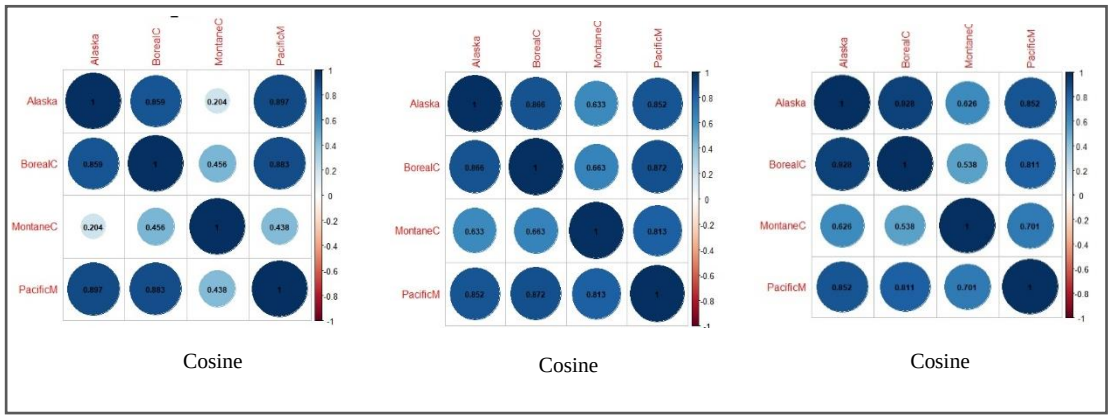

Appendix IV, Glacier surface albedo (a) and Glacier surface temperature (b) Cosine similarity in the 4 main ecozone of the study area for June, July and August over 21 years (2000-2020)

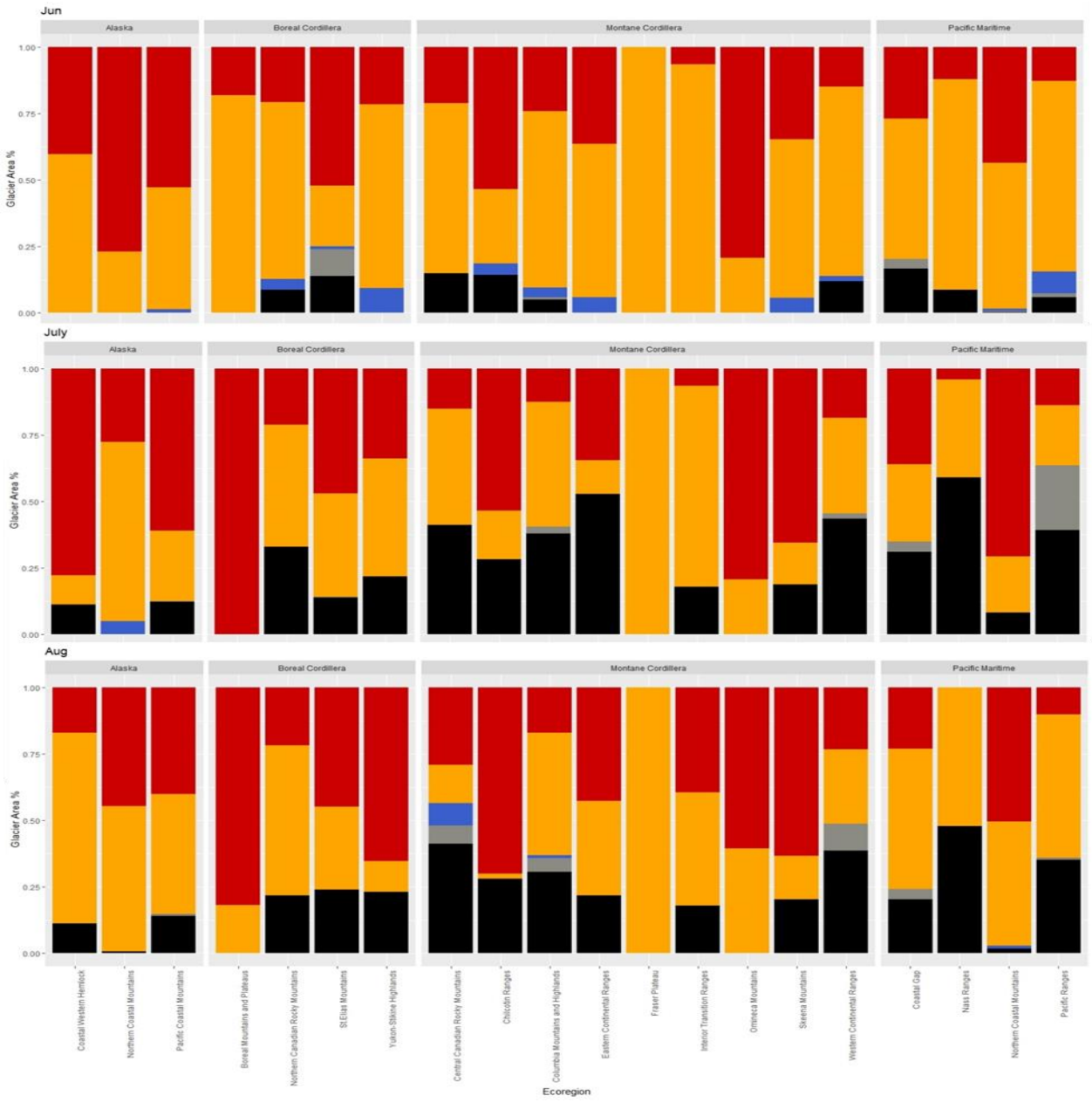

Appendix V, Results from the combine glacier surface temperature and albedo significant trends by glaciated areas of the 20 ecoregions. "Red color illustrates the glaciated areas with positive significant trend in surface temperature AND negative significant trend in albedo, orange color represents the glaciated areas with positive significant trend in surface temperature OR negative significant trend in albedo, the blue color represents the area of glaciers the surface temperature decline and surface albedo increase, the grey color represents the glaciated areas the trends are not significant and the black color illustrates the glaciated areas with missing data".

Appendix VI, Glacier surface albedo anomalies and surface temperature °C anomalies in the 4 main ecozone of the study area for June, July and August over 21 years (2000-2020). In the column names, "A" indicates surface albedo and "T" indicates surface temperature

Glacier surface albedo and temperature anomalies																								
	Alaska						**Boreal Cordillera**						**Montane cordillera**						**Pacific Maritime**					
	June		July		August		June		July		August		June		July		August		June		July		August	
	A	T	A	T	A	T	A	T	A	T	A	T	A	T	A	T	A	T	A	T	A	T	A	T
2000	0.02	0.66	-0.01	0.28	0.04	0.30	0.03	0.55	0.05	0.76	0.03	0.73	0.01	0.67	0.04	0.43	0.04	0.93	0.02	0.50	0.03	0.38	0.06	0.11
2001	0.02	0.20	0.05	0.60	0.05	0.57	0.02	0.17	0.10	0.69	0.04	0.77	0.03	0.23	0.03	0.22	0.04	0.66	0.04	0.41	0.04	0.08	0.04	0.20
2002	-0.03	-0.05	-0.06	0.39	-0.07	0.46	-0.03	-0.03	-0.04	0.55	-0.04	0.37	-0.02	-0.19	-0.01	0.75	-0.01	0.69	-0.02	0.12	0.00	1.21	-0.04	0.73
2003	-0.08	0.83	-0.12	0.77	-0.08	0.35	-0.12	0.71	-0.08	0.75	-0.05	0.74	-0.04	0.53	-0.05	0.72	-0.04	0.88	-0.03	0.60	-0.05	0.66	-0.04	1.29
2004	-0.03	1.03	-0.04	0.68	-0.08	1.25	-0.03	0.89	-0.03	0.48	-0.07	1.50	-0.05	0.85	-0.06	0.28	-0.07	1.15	-0.05	1.05	-0.04	0.29	-0.07	1.42
2005	-0.03	1.05	-0.09	0.04	-0.09	1.15	-0.03	0.88	-0.09	-0.16	-0.04	1.06	-0.02	0.85	-0.05	0.22	-0.06	0.63	-0.02	0.54	-0.03	-0.01	-0.04	0.85
2006	-0.08	0.51	0.01	0.64	0.01	0.70	-0.02	0.76	0.00	0.56	-0.16	0.21	-0.01	0.88	0.02	0.40	-0.05	0.55	-0.02	0.74	0.01	0.01	-0.01	1.16
2007	0.00	0.33	0.00	-0.42	-0.03	0.94	0.01	0.14	-0.02	0.64	-0.02	1.09	0.01	0.33	0.04	0.32	0.04	0.42	0.00	0.27	0.01	0.74	0.04	1.37
2008	-0.01	-0.12	-0.03	-0.33	-0.04	-0.58	-0.01	0.18	0.00	-0.64	-0.01	0.09	-0.01	0.33	0.02	0.28	0.05	0.07	0.00	0.13	0.01	-0.16	0.02	0.37
2009	0.00	0.27	-0.02	0.90	-0.03	-1.06	0.00	0.52	0.01	0.97	-0.02	-0.99	0.00	0.77	0.00	0.73	-0.03	-0.18	0.00	0.66	0.00	0.98	-0.01	0.12
2010	-0.01	0.27	-0.06	0.41	-0.01	0.91	-0.03	0.01	0.00	0.65	-0.05	1.32	-0.02	0.52	-0.01	0.20	-0.03	0.84	-0.02	0.11	-0.02	0.64	-0.05	0.62
2011	-0.04	0.14	-0.02	0.42	0.08	0.47	-0.07	0.41	-0.05	0.33	-0.06	0.06	-0.03	0.38	-0.09	-0.34	-0.01	0.20	-0.03	0.60	-0.03	0.25	0.04	0.25
2012	0.06	-0.23	0.04	0.26	0.10	0.66	0.02	-0.18	0.08	-0.27	0.10	0.67	0.01	-0.10	0.04	0.12	0.07	0.98	0.02	0.25	0.04	-0.03	0.06	0.58
2013	-0.01	0.74	-0.07	0.81	-0.06	0.76	0.00	0.72	-0.05	0.90	-0.06	1.26	-0.02	0.54	-0.04	0.92	-0.06	1.01	-0.01	0.53	-0.04	0.28	-0.07	1.13
2014	-0.07	0.64	-0.09	0.94	-0.11	1.08	-0.03	0.53	-0.07	0.68	-0.10	0.81	-0.01	0.67	-0.03	0.60	-0.07	0.76	-0.01	0.75	-0.04	0.65	-0.08	0.29

2015	-0.07	1.21	-0.08	0.41	-0.10	0.60	-0.09	0.85	-0.15	0.99	-0.06	0.61	-0.08	1.04	-0.09	0.34	-0.08	0.47	-0.05	1.11	-0.03	0.56	-0.07	1.51
2016	-0.05	1.01	-0.07	0.87	-0.10	0.46	-0.05	0.63	-0.05	0.62	-0.06	0.99	-0.06	0.60	-0.08	0.57	-0.09	0.97	-0.03	0.67	-0.04	0.82	-0.10	1.19
2017	-0.02	-0.29	0.00	-0.82	-0.06	-0.40	-0.06	0.16	-0.03	0.39	-0.05	-0.73	-0.03	0.44	-0.03	0.68	-0.06	-1.27	-0.03	0.03	-0.01	0.43	-0.08	-1.26
2018	-0.02	-0.40	-0.14	1.15	-0.11	0.62	-0.12	-0.56	-0.13	1.03	-0.09	0.40	-0.08	-0.21	-0.11	0.90	-0.15	1.01	-0.05	-0.45	-0.15	1.07	-0.14	0.88
2019	-0.12	1.09	-0.16	0.16	-0.14	1.01	-0.15	0.91	-0.14	0.45	-0.11	1.18	-0.12	0.45	-0.15	0.66	-0.13	1.15	-0.10	0.91	-0.15	0.57	-0.14	1.24
2020	0.00	-0.18	0.00	0.86	-0.01	0.81	-0.01	0.21	-0.01	-0.59	-0.11	0.40	-0.01	-0.25	0.01	-0.57	-0.03	-0.58	0.00	-0.22	-0.02	0.37	0.02	-0.23
Average	**-0.03**	**0.41**	**-0.05**	**0.43**	**-0.04**	**0.53**	**-0.04**	**0.40**	**-0.03**	**0.46**	**-0.05**	**0.60**	**-0.02**	**0.44**	**-0.03**	**0.40**	**-0.04**	**0.54**	**-0.02**	**0.44**	**-0.02**	**0.47**	**-0.03**	**0.66**

Appendix VII, Overview of the Canadian Rocky mountain glaciers with significant albedo decrease and temperature increase over 21 years (2000-2020)

Number	RGIID	Longitude (Centre)	Latitude (Centre)	Area Km2	Elevation m.a.s.l			Slope (%)	Aspect	Length	Ecozone	Ecoregion
					Min	Max	Median					
1	RGI60-02.01200	-116.7	50.5	5.062	2224	2867	2595	10.7	94	4842	Montane Cordillera	Columbia Mountains and Highlands
2	RGI60-02.01592	-116.9	50.6	3.351	2098	2965	2576	16.7	349	2942	Montane Cordillera	Columbia Mountains and Highlands
3	RGI60-02.03686	-117.4	51.2	13.452	1879	2782	2547	10	233	4684	Montane Cordillera	Columbia Mountains and Highlands
4	RGI60-02.05515	-116.9	51.7	37.98	1623	3263	2619	13.1	356	12276	Montane Cordillera	Western Continental Ranges
5	RGI60-02.05825	-118.2	51.9	8.9	1548	3067	2546	16.6	319	5965	Montane Cordillera	Columbia Mountains and Highlands
6	RGI60-02.05938	-118.1	51.9	4.927	1865	2757	2369	17.3	339	4071	Montane Cordillera	Columbia Mountains and Highlands
7	RGI60-02.06380	-117.8	52.0	10.022	1759	2967	2463	15.8	135	6634	Montane Cordillera	Western Continental Ranges
8	RGI60-02.06428	-118.9	52.1	4.456	1885	2643	2337	13.6	143	4026	Montane Cordillera	Columbia Mountains and Highlands
9	RGI60-02.06520	-117.8	52.1	5.507	1719	2995	2383	17.3	9	5023	Montane Cordillera	Western Continental Ranges
10	RGI60-02.06558	-117.6	52.1	10.98	1663	3022	2622	15.6	134	5409	Montane Cordillera	Western Continental Ranges
11	RGI60-02.06860	-117.9	52.2	43.951	1314	3063	2503	14.4	174	10791	Montane Cordillera	Western Continental Ranges
12	RGI60-02.06862	-117.9	52.2	20.588	1627	3134	2471	13.9	331	9549	Montane Cordillera	Western Continental Ranges
13	RGI60-02.06929	-117.2	52.1	30.386	1820	3283	2622	10.2	110	12748	Montane Cordillera	Eastern Continental Ranges
14	RGI60-02.07601	-120.0	52.5	5.721	2051	2627	2446	9.6	111	2438	Montane Cordillera	Columbia Mountains and Highlands
15	RGI60-02.07657	-119.9	52.6	3.204	1908	2591	2377	13.8	24	3137	Montane Cordillera	Columbia Mountains and Highlands
16	RGI60-02.08511	-120.2	52.9	26.612	1593	2790	2328	9.6	299	9281	Montane Cordillera	Columbia Mountains and Highlands
17	RGI60-02.08769	-120.5	53.0	12.975	1688	2885	2317	11.5	136	5811	Montane Cordillera	Columbia Mountains and Highlands
18	RGI60-02.08783	-120.5	53.0	9.664	1835	2785	2399	11.1	27	6228	Montane Cordillera	Columbia Mountains and Highlands
19	RGI60-02.09027	-119.1	53.1	11.428	1703	3513	2457	19.2	20	7523	Montane Cordillera	Western Continental Ranges
20	RGI60-02.09099	-120.5	53.2	6.536	2011	2610	2246	10.3	74	3788	Montane Cordillera	Columbia Mountains and Highlands
21	RGI60-02.09255	-119.3	53.2	7.94	2060	3024	2454	13.1	51	4794	Montane Cordillera	Western Continental Ranges
22	RGI60-02.09720	-119.5	53.4	26.781	1721	3285	2526	11.8	91	8988	Montane Cordillera	Eastern Continental Ranges
23	RGI60-02.12433	-117.6	52.2	11.332	2066	3018	2629	10.5	304	6213	Montane Cordillera	Western Continental Ranges
24	RGI60-02.12435	-117.3	52.1	16.769	1614	3285	2690	9.5	184	7711	Montane Cordillera	Western Continental Ranges

25	RGI60-02.12437	-117.4	52.2	29.983	1550	3638	2883	14.7	249	9285	Montane Cordillera	Western Continental Ranges
26	RGI60-02.12440	-117.4	52.1	10.877	1861	3040	2671	13.2	146	6062	Montane Cordillera	Western Continental Ranges
27	RGI60-02.12441	-117.3	52.2	16.154	1982	3448	2870	12.6	93	10396	Montane Cordillera	Western Continental Ranges
28	RGI60-02.12443	-117.4	52.1	3.734	1558	2841	2632	18.9	182	4081	Montane Cordillera	Western Continental Ranges
29	RGI60-02.12444	-117.4	52.2	19.613	1724	3462	3129	16.6	24	7129	Montane Cordillera	Eastern Continental Ranges

Appendix VIII, The percentage of airflow trajectories reaching the glaciers as determined through Back Trajectory Analyses

Number	RGIID	Anomalously Year	Simulation period	June				July				August			
				North	East	South	West	North	East	South	West	North	East	South	West
1	RGI60-02.01200	2017	Week 01	15	8	9	68	14	8.5	10	69	16	12	11	63
1	RGI60-02.01200	2017	Week 02	10	7	12	71	9	7.5	13	72	11	11	14	66
1	RGI60-02.01200	2017	Week 03	18	10	10	62	17	10.5	11	63	19	14	12	57
1	RGI60-02.01200	2017	Week 04	15	8	5	72	14	8.5	6	73	16	12	7	67
1	RGI60-02.01200	2019	Week 01	12	13	15	60	11	13.5	16	61	13	17	17	55
1	RGI60-02.01200	2019	Week 02	5	7	8	80	4	7.5	9	81	6	11	10	75
1	RGI60-02.01200	2019	Week 03	5	5	10	80	4	5.5	11	81	6	9	12	75
1	RGI60-02.01200	2019	Week 04	15	0	0	85	14	0.5	1	86	16	4	2	80
2	RGI60-02.01592	2017	Week 01	10	0	10	80	9	0.5	11	81	11	4	12	75
2	RGI60-02.01592	2017	Week 02	8	1	7	84	7	1.5	8	85	9	5	9	79
2	RGI60-02.01592	2017	Week 03	10	13	7	70	9	13.5	8	71	11	17	9	65
2	RGI60-02.01592	2017	Week 04	20	10	5	65	19	10.5	6	66	21	14	7	60
2	RGI60-02.01592	2019	Week 01	7	3	5	85	6	3.5	6	86	8	7	7	80
2	RGI60-02.01592	2019	Week 02	12	8	4	76	11	8.5	5	77	13	12	6	71
2	RGI60-02.01592	2019	Week 03	20	10	9	61	19	10.5	10	62	21	14	11	56
2	RGI60-02.01592	2019	Week 04	17	8	5	70	16	8.5	6	71	18	12	7	65
3	RGI60-02.03686	2017	Week 01	7	8	5	80	6	8.5	6	81	8	12	7	75
3	RGI60-02.03686	2017	Week 02	17	5	3	75	16	5.5	4	76	18	9	5	70
3	RGI60-02.03686	2017	Week 03	2	3	5	90	1	3.5	6	91	3	7	7	85
3	RGI60-02.03686	2017	Week 04	6	8		86	5	8.5	1	87	7	12	2	81
3	RGI60-02.03686	2019	Week 01	15	5		80	14	5.5	1	81	16	9	2	75
3	RGI60-02.03686	2019	Week 02	10	5	2	83	9	5.5	3	84	11	9	4	78
3	RGI60-02.03686	2019	Week 03	5	2	1	91	4	2.5	2	92	6	6	3	86
3	RGI60-02.03686	2019	Week 04	7		3	90	6	0.5	4	91	8	4	5	85

4	RGI60-02.05515	2017	Week 01	20	5	5	70	19	5.5	6	71	21	9	7	65
4	RGI60-02.05515	2017	Week 02	16	3	1	80	15	3.5	2	81	17	7	3	75
4	RGI60-02.05515	2017	Week 03	3	10	2	85	2	10.5	3	86	4	14	4	80
4	RGI60-02.05515	2017	Week 04	5	1		94	4	1.5	1	95	6	5	2	89
4	RGI60-02.05515	2019	Week 01	15	8	2	75	14	8.5	3	76	16	12	4	70
4	RGI60-02.05515	2019	Week 02	15	9		76	14	9.5	1	77	16	13	2	71
4	RGI60-02.05515	2019	Week 03	5	4	1	90	4	4.5	2	91	6	8	3	85
4	RGI60-02.05515	2019	Week 04	13	5	2	80	12	5.5	3	81	14	9	4	75
5	RGI60-02.05825	2017	Week 01	20	5	1	74	19	5.5	2	75	21	9	3	69
5	RGI60-02.05825	2017	Week 02	18	12	5	65	17	12.5	6	66	19	16	7	60
5	RGI60-02.05825	2017	Week 03	15	8	2	75	14	8.5	3	76	16	12	4	70
5	RGI60-02.05825	2017	Week 04	10	5	5	80	9	5.5	6	81	11	9	7	75
5	RGI60-02.05825	2019	Week 01	7	2		91	6	2.5	1	92	8	6	2	86
5	RGI60-02.05825	2019	Week 02	10	8	2	80	9	8.5	3	81	11	12	4	75
5	RGI60-02.05825	2019	Week 03	6	3	1	90	5	3.5	2	91	7	7	3	85
5	RGI60-02.05825	2019	Week 04	10	2	3	85	9	2.5	4	86	11	6	5	80
6	RGI60-02.05938	2017	Week 01	10	5	10	75	9	5.5	11	76	11	9	12	70
6	RGI60-02.05938	2017	Week 02	12	8		86	11	8.5	1	87	13	12	2	81
6	RGI60-02.05938	2017	Week 03	5	2	3	90	4	2.5	4	91	6	6	5	85
6	RGI60-02.05938	2017	Week 04	14	8	3	75	13	8.5	4	76	15	12	5	70
6	RGI60-02.05938	2019	Week 01	15			85	14	0.5	1	86	16	4	2	80
6	RGI60-02.05938	2019	Week 02	7	3		90	6	3.5	1	91	8	7	2	85
6	RGI60-02.05938	2019	Week 03	10		2	88	9	0.5	3	89	11	4	4	83
6	RGI60-02.05938	2019	Week 04	5	5		90	4	5.5	1	91	6	9	2	85
7	RGI60-02.06380	2017	Week 01	15	4	1	80	14	4.5	2	81	16	8	3	75
7	RGI60-02.06380	2017	Week 02	10	4		86	9	4.5	1	87	11	8	2	81
7	RGI60-02.06380	2017	Week 03	8	2	6	84	7	2.5	7	85	9	6	8	79
7	RGI60-02.06380	2017	Week 04	18	10	2	70	17	10.5	3	71	19	14	4	65
7	RGI60-02.06380	2019	Week 01	10	10	0	80	9	10.5	1	81	11	14	2	75
7	RGI60-02.06380	2019	Week 02	5	1		94	4	1.5	1	95	6	5	2	89

7	RGI60-02.06380	2019	Week 03	6	2		92	5	2.5	1	93	7	6	2	87
7	RGI60-02.06380	2019	Week 04	12	6	2	80	11	6.5	3	81	13	10	4	75
8	RGI60-02.06428	2017	Week 01	15	8	2	75	14	8.5	3	76	16	12	4	70
8	RGI60-02.06428	2017	Week 02	8	4	3	85	7	4.5	4	86	9	8	5	80
8	RGI60-02.06428	2017	Week 03	14			86	13	0.5	1	87	15	4	2	81
8	RGI60-02.06428	2017	Week 04	40			60	39	0.5	1	61	41	4	2	55
8	RGI60-02.06428	2019	Week 01	25	8	2	65	24	8.5	3	66	26	12	4	60
8	RGI60-02.06428	2019	Week 02	22			78	21	0.5	1	79	23	4	2	73
8	RGI60-02.06428	2019	Week 03	10		4	86	9	0.5	5	87	11	4	6	81
8	RGI60-02.06428	2019	Week 04	5			95	4	0.5	1	96	6	4	2	90
9	RGI60-02.06520	2017	Week 01	20	7		73	19	7.5	1	74	21	11	2	68
9	RGI60-02.06520	2017	Week 02	23			77	22	0.5	1	78	24	4	2	72
9	RGI60-02.06520	2017	Week 03	6			94	5	0.5	1	95	7	4	2	89
9	RGI60-02.06520	2017	Week 04	12		3	85	11	0.5	4	86	13	4	5	80
9	RGI60-02.06520	2019	Week 01	5		5	90	4	0.5	6	91	6	4	7	85
9	RGI60-02.06520	2019	Week 02	12	2		86	11	2.5	1	87	13	6	2	81
9	RGI60-02.06520	2019	Week 03	8	6	1	85	7	6.5	2	86	9	10	3	80
9	RGI60-02.06520	2019	Week 04	25	5	2	68	24	5.5	3	69	26	9	4	63
10	RGI60-02.06558	2017	Week 01	18	1	10	71	17	1.5	11	72	19	5	12	66
10	RGI60-02.06558	2017	Week 02	17	8		75	16	8.5	1	76	18	12	2	70
10	RGI60-02.06558	2017	Week 03	5	2	3	90	4	2.5	4	91	6	6	5	85
10	RGI60-02.06558	2017	Week 04	6	10		84	5	10.5	1	85	7	14	2	79
10	RGI60-02.06558	2019	Week 01	26	2	8	64	25	2.5	9	65	27	6	10	59
10	RGI60-02.06558	2019	Week 02	24		3	73	23	0.5	4	74	25	4	5	68
10	RGI60-02.06558	2019	Week 03	19		3	78	18	0.5	4	79	20	4	5	73
10	RGI60-02.06558	2019	Week 04	15	16	4	65	14	16.5	5	66	16	20	6	60
11	RGI60-02.06860	2017	Week 01	19	6	10	66	18	6.5	11	67	20	10	12	61
11	RGI60-02.06860	2017	Week 02	10	20		70	9	20.5	1	71	11	24	2	65
11	RGI60-02.06860	2017	Week 03	16	10		74	15	10.5	1	75	17	14	2	69
11	RGI60-02.06860	2017	Week 04	8	18		75	7	18.5	1	76	9	22	2	70

11	RGI60-02.06860	2019	Week 01	6	4		90	5	4.5	1	91	7	8	2	85
11	RGI60-02.06860	2019	Week 02	25			76	24	0.5	1	77	26	4	2	71
11	RGI60-02.06860	2019	Week 03	20	9		71	19	9.5	1	72	21	13	2	66
11	RGI60-02.06860	2019	Week 04	18	22	10	50	17	22.5	11	51	19	26	12	45
12	RGI60-02.06862	2017	Week 01	15	14	1	70	14	14.5	2	71	16	18	3	65
12	RGI60-02.06862	2017	Week 02	10	5		85	9	5.5	1	86	11	9	2	80
12	RGI60-02.06862	2017	Week 03	18	12	6	65	17	12.5	7	66	19	16	8	60
12	RGI60-02.06862	2017	Week 04	17	10	2	90	16	10.5	3	91	18	14	4	85
12	RGI60-02.06862	2019	Week 01	12	10	0	78	11	10.5	1	79	13	14	2	73
12	RGI60-02.06862	2019	Week 02	15	1		84	14	1.5	1	85	16	5	2	79
12	RGI60-02.06862	2019	Week 03	8	2		90	7	2.5	1	91	9	6	2	85
12	RGI60-02.06862	2019	Week 04	11	6	2	81	10	6.5	3	82	12	10	4	76
13	RGI60-02.06929	2017	Week 01	10	0	5	85	9	0.5	6	86	11	4	7	80
13	RGI60-02.06929	2017	Week 02	8	1	5	76	7	1.5	6	77	9	5	7	71
13	RGI60-02.06929	2017	Week 03	7	3	0	90	6	3.5	1	91	8	7	2	85
13	RGI60-02.06929	2017	Week 04	15	5	0	80	14	5.5	1	81	16	9	2	75
13	RGI60-02.06929	2019	Week 01	7	3	5	85	6	3.5	6	86	8	7	7	80
13	RGI60-02.06929	2019	Week 02	12	8	4	76	11	8.5	5	77	13	12	6	71
13	RGI60-02.06929	2019	Week 03	20	10	9	61	19	10.5	10	62	21	14	11	56
13	RGI60-02.06929	2019	Week 04	17	8	5	70	16	8.5	6	71	18	12	7	65
14	RGI60-02.07601	2017	Week 01	20	5	0	75	19	5.5	1	76	21	9	2	70
14	RGI60-02.07601	2017	Week 02	12	2		86	11	2.5	1	87	13	6	2	81
14	RGI60-02.07601	2017	Week 03	8	7	0	85	7	7.5	1	86	9	11	2	80
14	RGI60-02.07601	2017	Week 04	14	8	3	75	13	8.5	4	76	15	12	5	70
14	RGI60-02.07601	2019	Week 01	15			85	14	0.5	1	86	16	4	2	80
14	RGI60-02.07601	2019	Week 02	25	10		65	24	10.5	1	66	26	14	2	60
14	RGI60-02.07601	2019	Week 03	13		2	85	12	0.5	3	86	14	4	4	80
14	RGI60-02.07601	2019	Week 04	10	5		85	9	5.5	1	86	11	9	2	80
15	RGI60-02.07657	2017	Week 01	15	8	9	68	14	8.5	10	69	16	12	11	63
15	RGI60-02.07657	2017	Week 02	10	7	12	71	9	7.5	13	72	11	11	14	66

15	RGI60-02.07657	2017	Week 03	18	10	10	62	17	10.5	11	63	19	14	12	57
15	RGI60-02.07657	2017	Week 04	15	8	5	72	14	8.5	6	73	16	12	7	67
15	RGI60-02.07657	2019	Week 01	12	13	15	60	11	13.5	16	61	13	17	17	55
15	RGI60-02.07657	2019	Week 02	5	7	8	80	4	7.5	9	81	6	11	10	75
15	RGI60-02.07657	2019	Week 03	5	5	10	80	4	5.5	11	81	6	9	12	75
15	RGI60-02.07657	2019	Week 04	15	0	0	85	14	0.5	1	86	16	4	2	80
16	RGI60-02.08511	2017	Week 01	29	1	10	60	28	1.5	11	61	30	5	12	55
16	RGI60-02.08511	2017	Week 02	17	3		80	16	3.5	1	81	18	7	2	75
16	RGI60-02.08511	2017	Week 03	0	2	3	95	-1	2.5	4	96	1	6	5	90
16	RGI60-02.08511	2017	Week 04	0	10	6	84	-1	10.5	7	85	1	14	8	79
16	RGI60-02.08511	2019	Week 01	21	2		77	20	2.5	1	78	22	6	2	72
16	RGI60-02.08511	2019	Week 02	24		1	75	23	0.5	2	76	25	4	3	70
16	RGI60-02.08511	2019	Week 03	20		0	80	19	0.5	1	81	21	4	2	75
16	RGI60-02.08511	2019	Week 04	11	16	4	69	10	16.5	5	70	12	20	6	64
17	RGI60-02.08769	2017	Week 01	10	5		85	9	5.5	1	86	11	9	2	80
17	RGI60-02.08769	2017	Week 02	10			90	9	0.5	1	91	11	4	2	85
17	RGI60-02.08769	2017	Week 03	15	7	3	75	14	7.5	4	76	16	11	5	70
17	RGI60-02.08769	2017	Week 04	20	8	5	67	19	8.5	6	68	21	12	7	62
17	RGI60-02.08769	2019	Week 01	15			85	14	0.5	1	86	16	4	2	80
17	RGI60-02.08769	2019	Week 02	10	0		90	9	0.5	1	91	11	4	2	85
17	RGI60-02.08769	2019	Week 03	8		0	92	7	0.5	1	93	9	4	2	87
17	RGI60-02.08769	2019	Week 04	10	5		85	9	5.5	1	86	11	9	2	80
18	RGI60-02.08783	2017	Week 01	10	0	10	80	9	0.5	11	81	11	4	12	75
18	RGI60-02.08783	2017	Week 02	23			87	22	0.5	1	88	24	4	2	82
18	RGI60-02.08783	2017	Week 03	25	5	5	65	24	5.5	6	66	26	9	7	60
18	RGI60-02.08783	2017	Week 04	12		3	85	11	0.5	4	86	13	4	5	80
18	RGI60-02.08783	2019	Week 01	10		5	80	9	0.5	6	81	11	4	7	75
18	RGI60-02.08783	2019	Week 02	8	2		90	7	2.5	1	91	9	6	2	85
18	RGI60-02.08783	2019	Week 03	0	5	0	95	-1	5.5	1	96	1	9	2	90
18	RGI60-02.08783	2019	Week 04	25	0	5	70	24	0.5	6	71	26	4	7	65

19	RGI60-02.09027	2017	Week 01	22	8	0	70	21	8.5	1	71	23	12	2	65
19	RGI60-02.09027	2017	Week 02	12	0	12	76	11	0.5	13	77	13	4	14	71
19	RGI60-02.09027	2017	Week 03	10		10	80	9	0.5	11	81	11	4	12	75
19	RGI60-02.09027	2017	Week 04	25	6	5	64	24	6.5	6	65	26	10	7	59
19	RGI60-02.09027	2019	Week 01	12	10	15	63	11	10.5	16	64	13	14	17	58
19	RGI60-02.09027	2019	Week 02	5	11	8	76	4	11.5	9	77	6	15	10	71
19	RGI60-02.09027	2019	Week 03	5	5	10	80	4	5.5	11	81	6	9	12	75
19	RGI60-02.09027	2019	Week 04	15	6	0	79	14	6.5	1	80	16	10	2	74
20	RGI60-02.09099	2017	Week 01	16	9	0	85	15	9.5	1	86	17	13	2	80
20	RGI60-02.09099	2017	Week 02	0	15	5	80	-1	15.5	6	81	1	19	7	75
20	RGI60-02.09099	2017	Week 03	10	7	10	73	9	7.5	11	74	11	11	12	68
20	RGI60-02.09099	2017	Week 04	14	5	6	75	13	5.5	7	76	15	9	8	70
20	RGI60-02.09099	2019	Week 01	12	10	0	78	11	10.5	1	79	13	14	2	73
20	RGI60-02.09099	2019	Week 02	10	10	4	76	9	10.5	5	77	11	14	6	71
20	RGI60-02.09099	2019	Week 03	0	15	5	80	-1	15.5	6	81	1	19	7	75
20	RGI60-02.09099	2019	Week 04	11	6	2	81	10	6.5	3	82	12	10	4	76
21	RGI60-02.09255	2017	Week 01	7	8	5	80	6	8.5	6	81	8	12	7	75
21	RGI60-02.09255	2017	Week 02	17	5	3	75	16	5.5	4	76	18	9	5	70
21	RGI60-02.09255	2017	Week 03	2	3	5	90	1	3.5	6	91	3	7	7	85
21	RGI60-02.09255	2017	Week 04	6	8		86	5	8.5	1	87	7	12	2	81
21	RGI60-02.09255	2019	Week 01	15	5		80	14	5.5	1	81	16	9	2	75
21	RGI60-02.09255	2019	Week 02	10	5	2	83	9	5.5	3	84	11	9	4	78
21	RGI60-02.09255	2019	Week 03	5	2	2	91	4	2.5	3	92	6	6	4	86
21	RGI60-02.09255	2019	Week 04	7		3	90	6	0.5	4	91	8	4	5	85
22	RGI60-02.09720	2017	Week 01	15	8	2	75	14	8.5	3	76	16	12	4	70
22	RGI60-02.09720	2017	Week 02	8	4	3	85	7	4.5	4	86	9	8	5	80
22	RGI60-02.09720	2017	Week 03	14			86	13	0.5	1	87	15	4	2	81
22	RGI60-02.09720	2017	Week 04	40			60	39	0.5	1	61	41	4	2	55
22	RGI60-02.09720	2019	Week 01	25	8	2	65	24	8.5	3	66	26	12	4	60
22	RGI60-02.09720	2019	Week 02	22			78	21	0.5	1	79	23	4	2	73

22	RGI60-02.09720	2019	Week 03	10		4	86	9	0.5	5	87	11	4	6	81
22	RGI60-02.09720	2019	Week 04	5			95	4	0.5	1	96	6	4	2	90
23	RGI60-02.12433	2017	Week 01	20	5	10	65	19	5.5	11	66	21	9	12	60
23	RGI60-02.12433	2017	Week 02	0	10	8	82	-1	10.5	9	83	1	14	10	77
23	RGI60-02.12433	2017	Week 03	3	3	4	90	2	3.5	5	91	4	7	6	85
23	RGI60-02.12433	2017	Week 04	10	9	5	76	9	9.5	6	77	11	13	7	71
23	RGI60-02.12433	2019	Week 01	5	3	7	85	4	3.5	8	86	6	7	9	80
23	RGI60-02.12433	2019	Week 02	12	8	4	84	11	8.5	5	85	13	12	6	79
23	RGI60-02.12433	2019	Week 03	10	1	7	82	9	1.5	8	83	11	5	9	77
23	RGI60-02.12433	2019	Week 04	17	8	5	70	16	8.5	6	71	18	12	7	65
24	RGI60-02.12435	2017	Week 01	10	4	1	85	9	4.5	2	86	11	8	3	80
24	RGI60-02.12435	2017	Week 02	11	14	10	65	10	14.5	11	66	12	18	12	60
24	RGI60-02.12435	2017	Week 03	3	1	6	90	2	1.5	7	91	4	5	8	85
24	RGI60-02.12435	2017	Week 04	18	5	2	75	17	5.5	3	76	19	9	4	70
24	RGI60-02.12435	2019	Week 01	12	5	0	83	11	5.5	1	84	13	9	2	78
24	RGI60-02.12435	2019	Week 02	5	3	1	91	4	3.5	2	92	6	7	3	86
24	RGI60-02.12435	2019	Week 03	16	4	6	74	15	4.5	7	75	17	8	8	69
24	RGI60-02.12435	2019	Week 04	10	6	0	84	9	6.5	1	85	11	10	2	79
25	RGI60-02.12437	2017	Week 01	10	8	6	76	9	8.5	7	77	11	12	8	71
25	RGI60-02.12437	2017	Week 02	1	2	2	95	0	2.5	3	96	2	6	4	90
25	RGI60-02.12437	2017	Week 03	14			86	13	0.5	1	87	15	4	2	81
25	RGI60-02.12437	2017	Week 04	40			60	39	0.5	1	61	41	4	2	55
25	RGI60-02.12437	2019	Week 01	10	4	2	84	9	4.5	3	85	11	8	4	79
25	RGI60-02.12437	2019	Week 02	22			78	21	0.5	1	79	23	4	2	73
25	RGI60-02.12437	2019	Week 03	10		4	86	9	0.5	5	87	11	4	6	81
25	RGI60-02.12437	2019	Week 04	5			95	4	0.5	1	96	6	4	2	90
26	RGI60-02.12440	2017	Week 01	11	5		84	10	5.5	1	85	12	9	2	79
26	RGI60-02.12440	2017	Week 02	23			77	22	0.5	1	78	24	4	2	72
26	RGI60-02.12440	2017	Week 03	10	2	20	68	9	2.5	21	69	11	6	22	63
26	RGI60-02.12440	2017	Week 04	10	5	15	70	9	5.5	16	71	11	9	17	65

26	RGI60-02.12440	2019	Week 01	5	4	5	86	4	4.5	6	87	6	8	7	81
26	RGI60-02.12440	2019	Week 02	12	2		86	11	2.5	1	87	13	6	2	81
26	RGI60-02.12440	2019	Week 03	11	8	1	80	10	8.5	2	81	12	12	3	75
26	RGI60-02.12440	2019	Week 04	10	5	3	82	9	5.5	4	83	11	9	5	77
27	RGI60-02.12441	2017	Week 01	20	0	10	70	19	0.5	11	71	21	4	12	65
27	RGI60-02.12441	2017	Week 02	17	3		80	16	3.5	1	81	18	7	2	75
27	RGI60-02.12441	2017	Week 03	5	2	3	90	4	2.5	4	91	6	6	5	85
27	RGI60-02.12441	2017	Week 04	0	7	9	84	-1	7.5	10	85	1	11	11	79
27	RGI60-02.12441	2019	Week 01	18	2		80	17	2.5	1	81	19	6	2	75
27	RGI60-02.12441	2019	Week 02	24		1	75	23	0.5	2	76	25	4	3	70
27	RGI60-02.12441	2019	Week 03	20	5	10	65	19	5.5	11	66	21	9	12	60
27	RGI60-02.12441	2019	Week 04	10	8	4	78	9	8.5	5	79	11	12	6	73
28	RGI60-02.12443	2017	Week 01	10	5		85	9	5.5	1	86	11	9	2	80
28	RGI60-02.12443	2017	Week 02	10			90	9	0.5	1	91	11	4	2	85
28	RGI60-02.12443	2017	Week 03	15	7	3	75	14	7.5	4	76	16	11	5	70
28	RGI60-02.12443	2017	Week 04	10	10	5	75	9	10.5	6	76	11	14	7	70
28	RGI60-02.12443	2019	Week 01	15		10	75	14	0.5	11	76	16	4	12	70
28	RGI60-02.12443	2019	Week 02	10	0		90	9	0.5	1	91	11	4	2	85
28	RGI60-02.12443	2019	Week 03	8		0	92	7	0.5	1	93	9	4	2	87
28	RGI60-02.12443	2019	Week 04	10	5	8	77	9	5.5	9	78	11	9	10	72
29	RGI60-02.12444	2017	Week 01	10	5	10	75	9	5.5	11	76	11	9	12	70
29	RGI60-02.12444	2017	Week 02	23	5	12	60	22	5.5	13	61	24	9	14	55
29	RGI60-02.12444	2017	Week 03	20	5	5	70	19	5.5	6	71	21	9	7	65
29	RGI60-02.12444	2017	Week 04	12		3	85	11	0.5	4	86	13	4	5	80
29	RGI60-02.12444	2019	Week 01	12	2	6	80	11	2.5	7	81	13	6	8	75
29	RGI60-02.12444	2019	Week 02	8	0		92	7	0.5	1	93	9	4	2	87
29	RGI60-02.12444	2019	Week 03	10	5	0	85	9	5.5	1	86	11	9	2	80
29	RGI60-02.12444	2019	Week 04	15	1	8	76	14	1.5	9	77	16	5	10	71

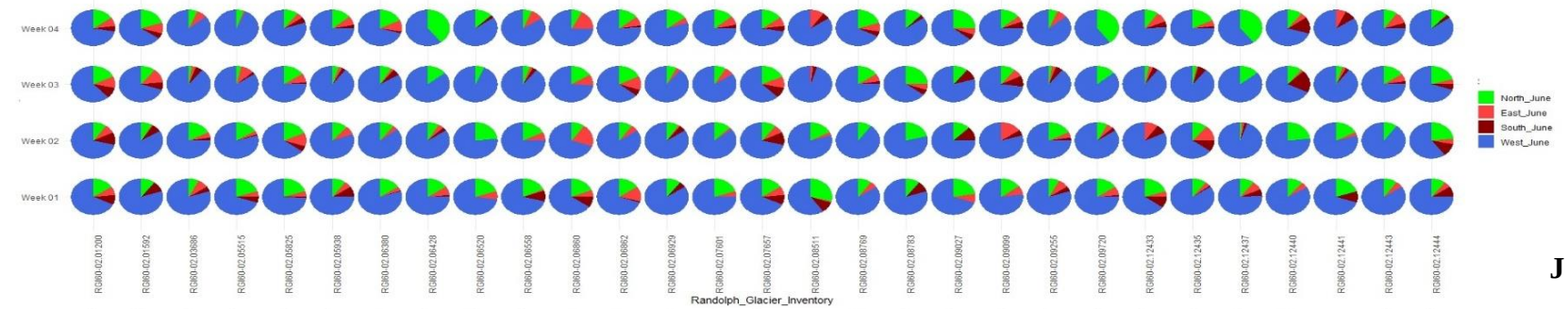
Week 04
Week 03
Week 02
Week 01
RGI60-02.01200
RGI60-02.01592
RGI60-02.03686
RGI60-02.05515
RGI60-02.05825
RGI60-02.05938
RGI60-02.06380
RGI60-02.06428
RGI60-02.06520
RGI60-02.06558
RGI60-02.06860
RGI60-02.06862
RGI60-02.06929
RGI60-02.07601
RGI60-02.07657
RGI60-02.08511
RGI60-02.08769
RGI60-02.08783
RGI60-02.09027
RGI60-02.09099
RGI60-02.09255
RGI60-02.09720
RGI60-02.12433
RGI60-02.12435
RGI60-02.12437
RGI60-02.12440
RGI60-02.12441
RGI60-02.12443
RGI60-02.12444
Randolph_Glacier_Inventory
North_June
East_June
South_June
West_June

J

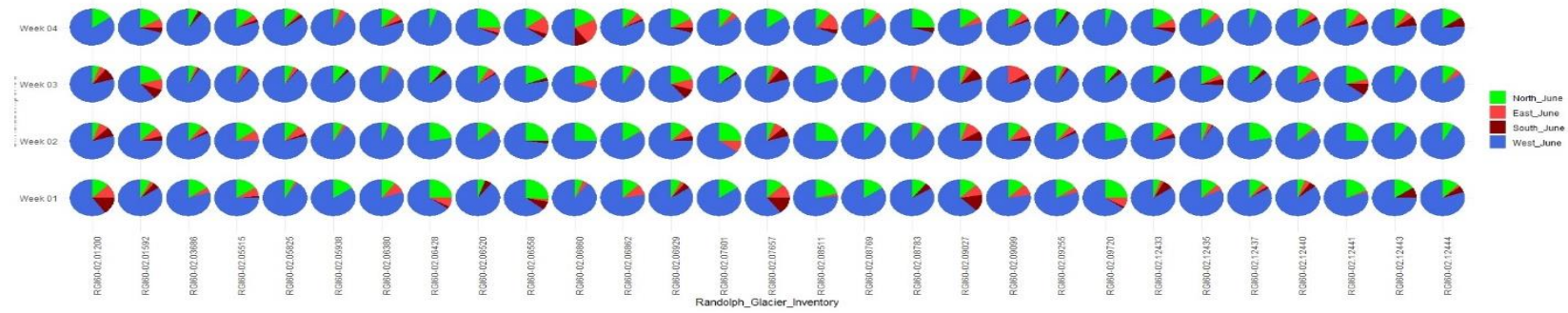
Week 04
Week 03
Week 02
Week 01
RGI60-02.01200
RGI60-02.01592
RGI60-02.03686
RGI60-02.05515
RGI60-02.05825
RGI60-02.05938
RGI60-02.06380
RGI60-02.06428
RGI60-02.06520
RGI60-02.06558
RGI60-02.06860
RGI60-02.06862
RGI60-02.06929
RGI60-02.07601
RGI60-02.07657
RGI60-02.08511
RGI60-02.08769
RGI60-02.08783
RGI60-02.09027
RGI60-02.09099
RGI60-02.09255
RGI60-02.09720
RGI60-02.12433
RGI60-02.12435
RGI60-02.12437
RGI60-02.12440
RGI60-02.12441
RGI60-02.12443
RGI60-02.12444
Randolph_Glacier_Inventory
North_June
East_June
South_June
West_June

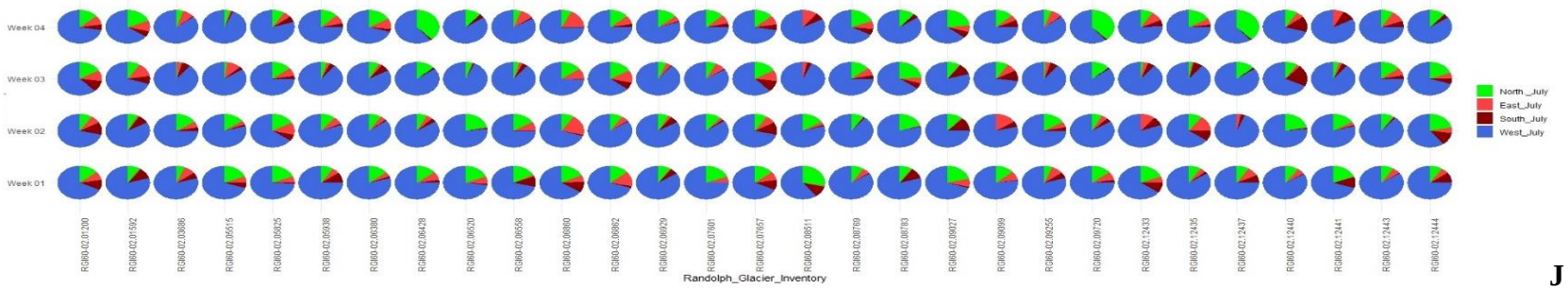
Week 04
Week 03
Week 02
Week 01
RGI60-02.01200
RGI60-02.01592
RGI60-02.03686
RGI60-02.05515
RGI60-02.05825
RGI60-02.05938
RGI60-02.06380
RGI60-02.06428
RGI60-02.06520
RGI60-02.06558
RGI60-02.06860
RGI60-02.06862
RGI60-02.06929
RGI60-02.07601
RGI60-02.07657
RGI60-02.08511
RGI60-02.08769
RGI60-02.08783
RGI60-02.09027
RGI60-02.09099
RGI60-02.09255
RGI60-02.09720
RGI60-02.12433
RGI60-02.12435
RGI60-02.12437
RGI60-02.12440
RGI60-02.12441
RGI60-02.12443
RGI60-02.12444
Randolph_Glacier_Inventory
North_July
East_July
South_July
West_July

J

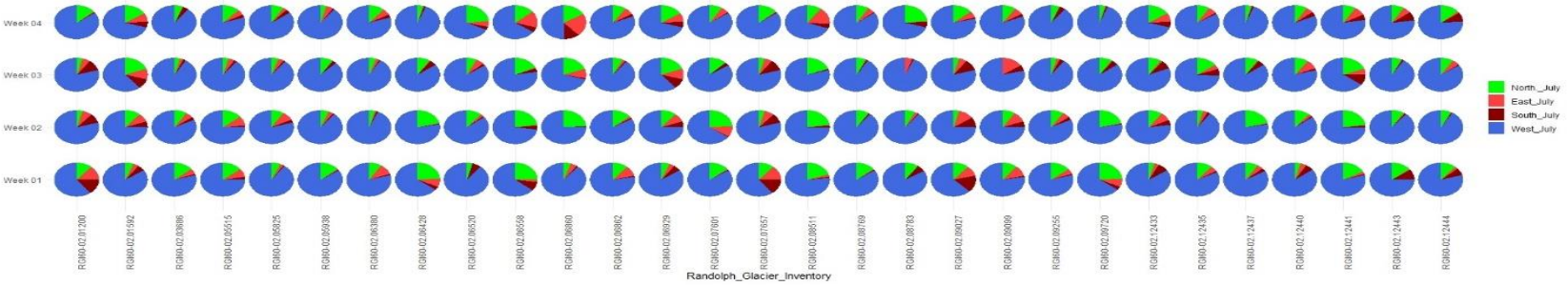
Week 04
Week 03
Week 02
Week 01
RGI60-02.01200
RGI60-02.01592
RGI60-02.03686
RGI60-02.05515
RGI60-02.05825
RGI60-02.05938
RGI60-02.06380
RGI60-02.06428
RGI60-02.06520
RGI60-02.06558
RGI60-02.06860
RGI60-02.06862
RGI60-02.06929
RGI60-02.07601
RGI60-02.07657
RGI60-02.08511
RGI60-02.08769
RGI60-02.08783
RGI60-02.09027
RGI60-02.09099
RGI60-02.09255
RGI60-02.09720
RGI60-02.12433
RGI60-02.12435
RGI60-02.12437
RGI60-02.12440
RGI60-02.12441
RGI60-02.12443
RGI60-02.12444
Randolph_Glacier_Inventory
North_July
East_July
South_July
West_July

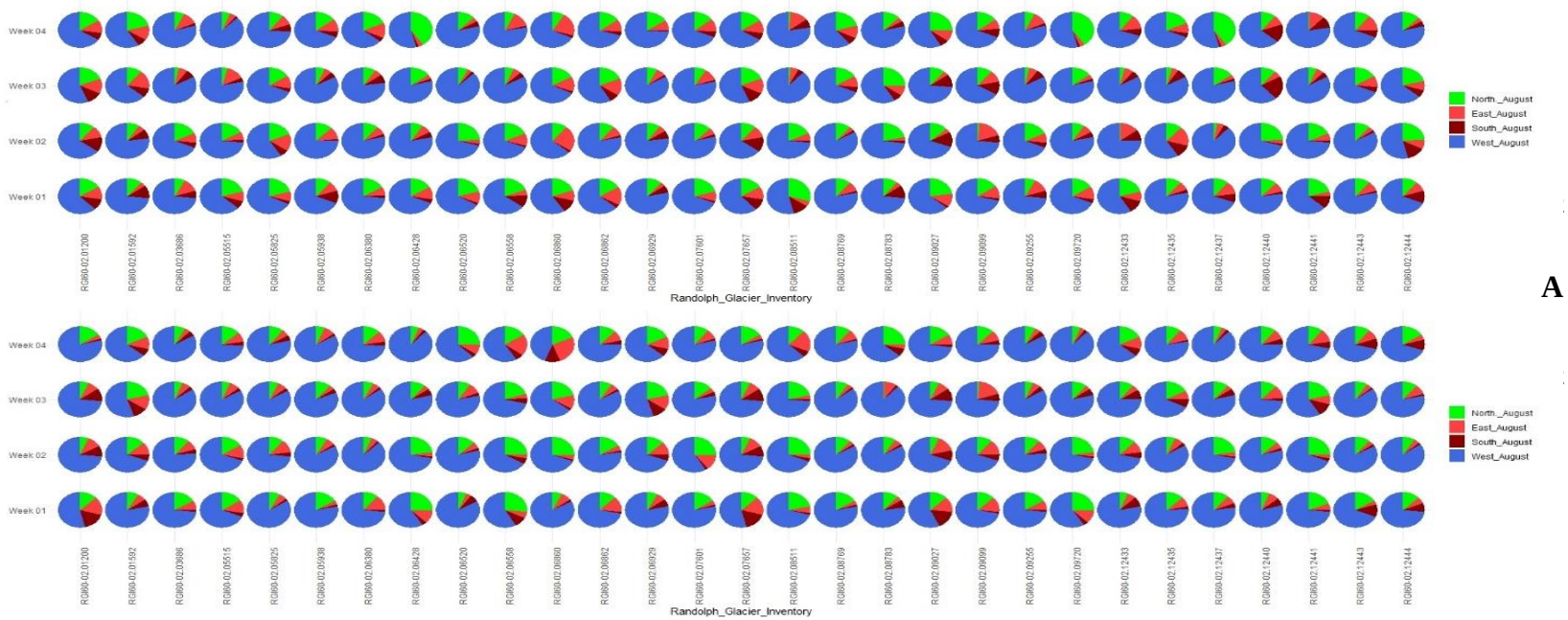

Appendix IX , Azimuth analyses of airflows that are reaching to the glaciers (29 glacier), x axis represent glaciers name by Randolph Glacier Inventory ID and y axis is indicating week of simulation of summer months (June, July and August)